Recent studies of heavy ion transfer reactions using large solid angle magnetic spectrometers

Suzana Szilner
Ruđer Bošković Institute, Zagreb
PRISMA collaboration

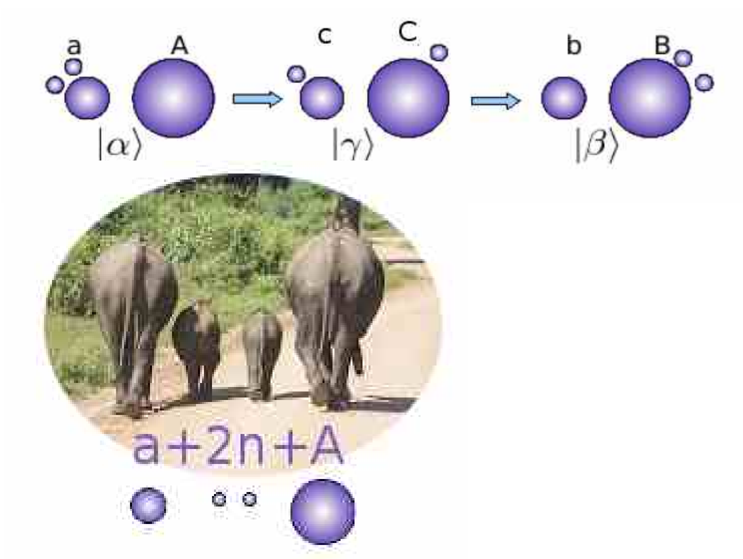

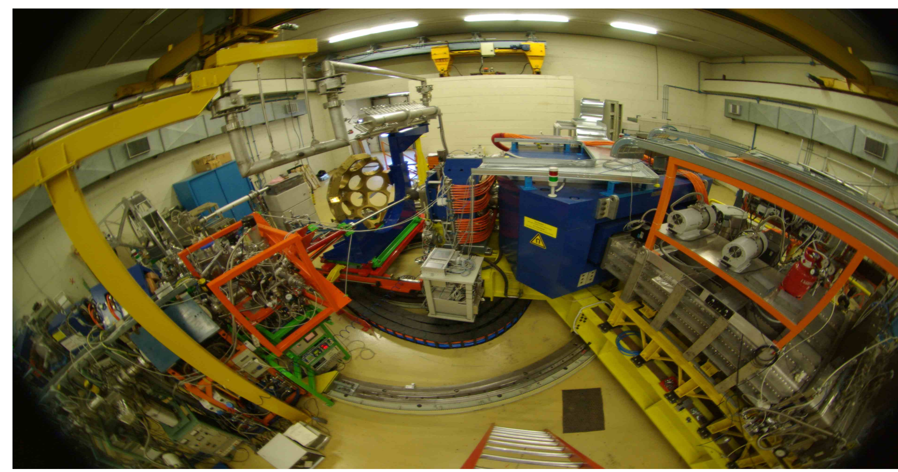

THE PRISMA + CLARA/AGATA CAMPAIGNS

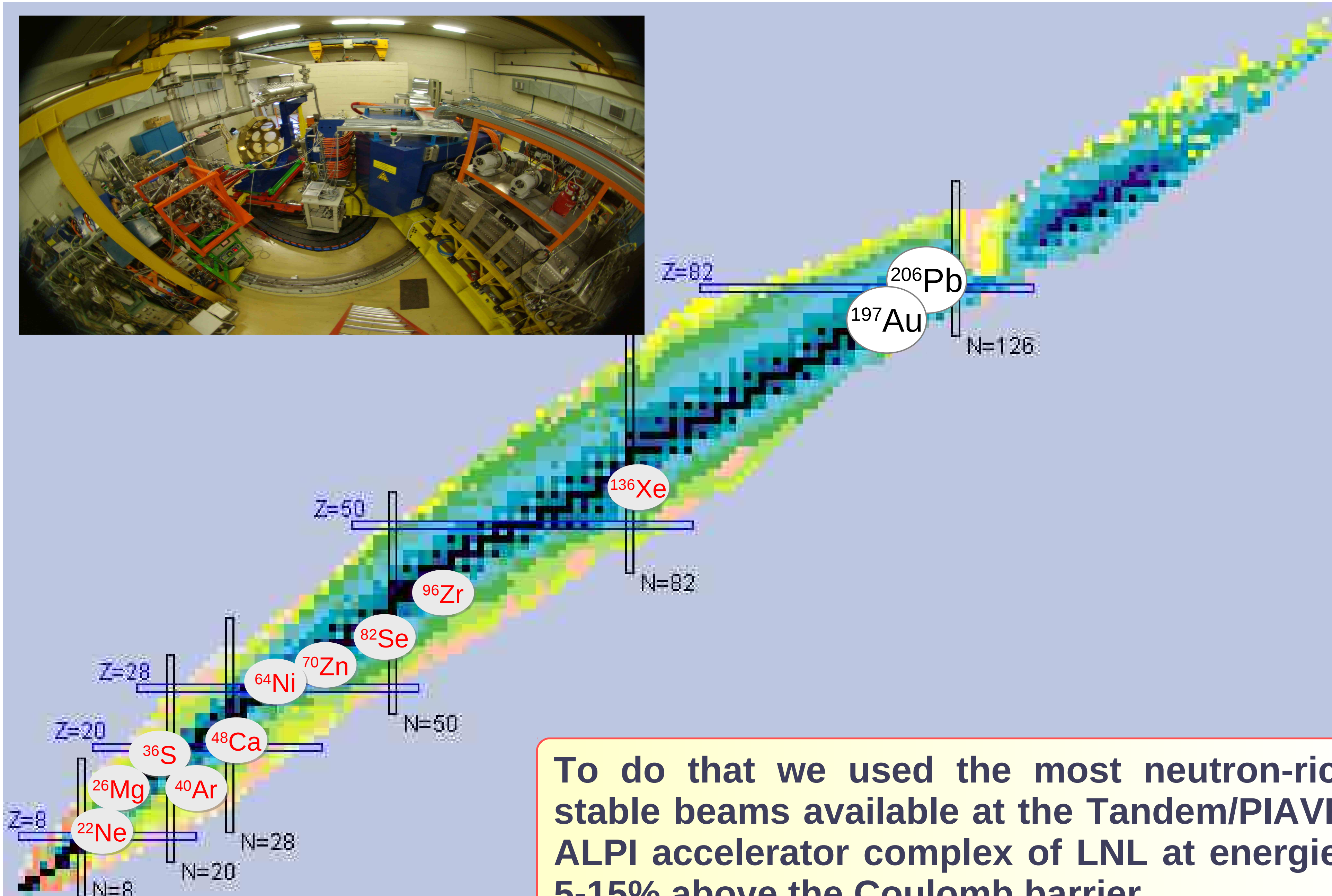

To do that we used the most neutron-rich stable beams available at the Tandem/PIAVE-ALPI accelerator complex of LNL at energies 5-15% above the Coulomb barrier

THE PRISMA + CLARA/AGATA CAMPAIGNS

L. Corradi, G. Pollarolo, F. Galtarossa, A. Goasduff, D. Montanari, E. Fioretto, A.M. Stefanini, G. Montagnoli, G. Coucci, F. Scarlassara, J.J. Valiente-Dobon, D. Mengoni, G. de Angelis, A. Gottardo, T. Marchi, D. Testov...
A. Illana, L.P. Gaffney, Th. Kroll ...
J. Diklić, T. Mijatović, P. Čolović, D. Jelavić Malenica, N. Soić, N. Vukman, M. Milin
AGATA collaboration

Ruđer Bošković Institute, Zagreb, Croatia
INFN - Laboratori Nazionali di Legnaro, Legnaro, Italy
INFN and Universita di Torino, Italy
INFN and Universita di Padova, Padova, Italy
University of Zagreb, Croatia
ISOLDE, CERN

Magnetic spectrometer PRISMA

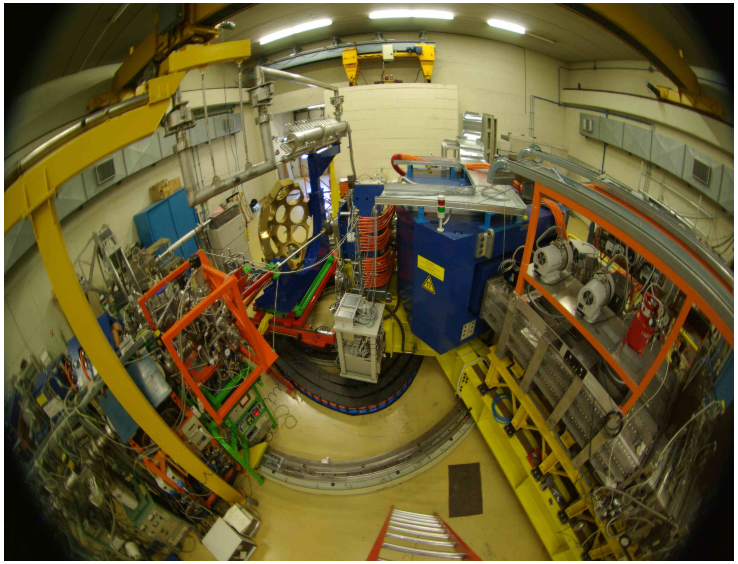

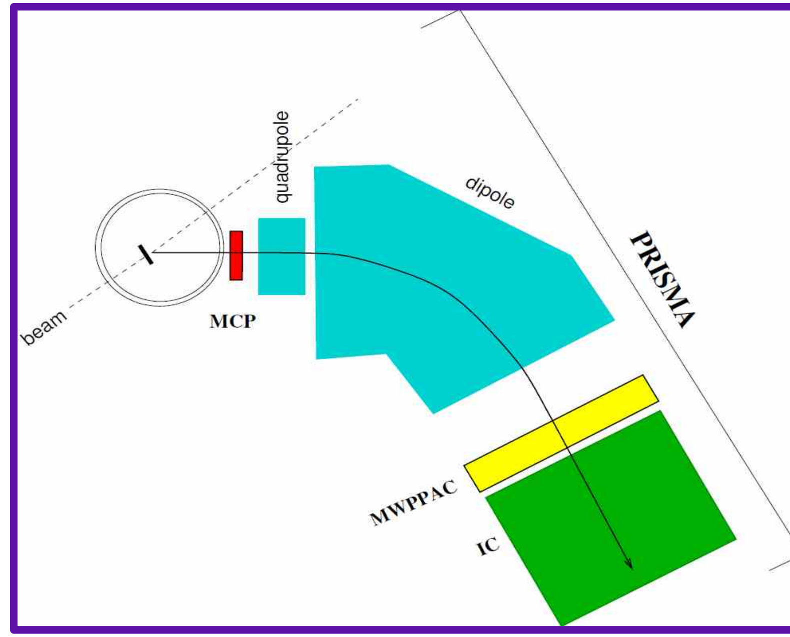

magnets: quadrupole + dipole
detectors:
start detector: MCP – micro-channel plate
focal plane detectors: MWPPAC – multiwire parallel plate avalanche counter, IC – ionization chamber

PRISMA:
$\Omega \approx$ 80 msr $B\rho_{max}$ = 1.2 Tm
$\Delta A/A \sim 1/200$
$\Delta Z/Z \sim 1/60$ for Z=20
E acceptance $\approx\pm20\%$

position in MCP: X_i, Y_i
focal plane position: x_f, y_f
Time of Flight: $ToF = t_f - t_i$
energy loss, total energy: ΔE, E - IC

→ **event-by-event trajectory reconstruction** →

A, q, Z, E, v
mass, charge, atomic state, energy, velocity

Heavy ion transfer reactions

Coulomb barrier energies

nucleon – nucleon correlations
studies of pairing in nuclei

studies of production of
heavy neutron-rich nuclei

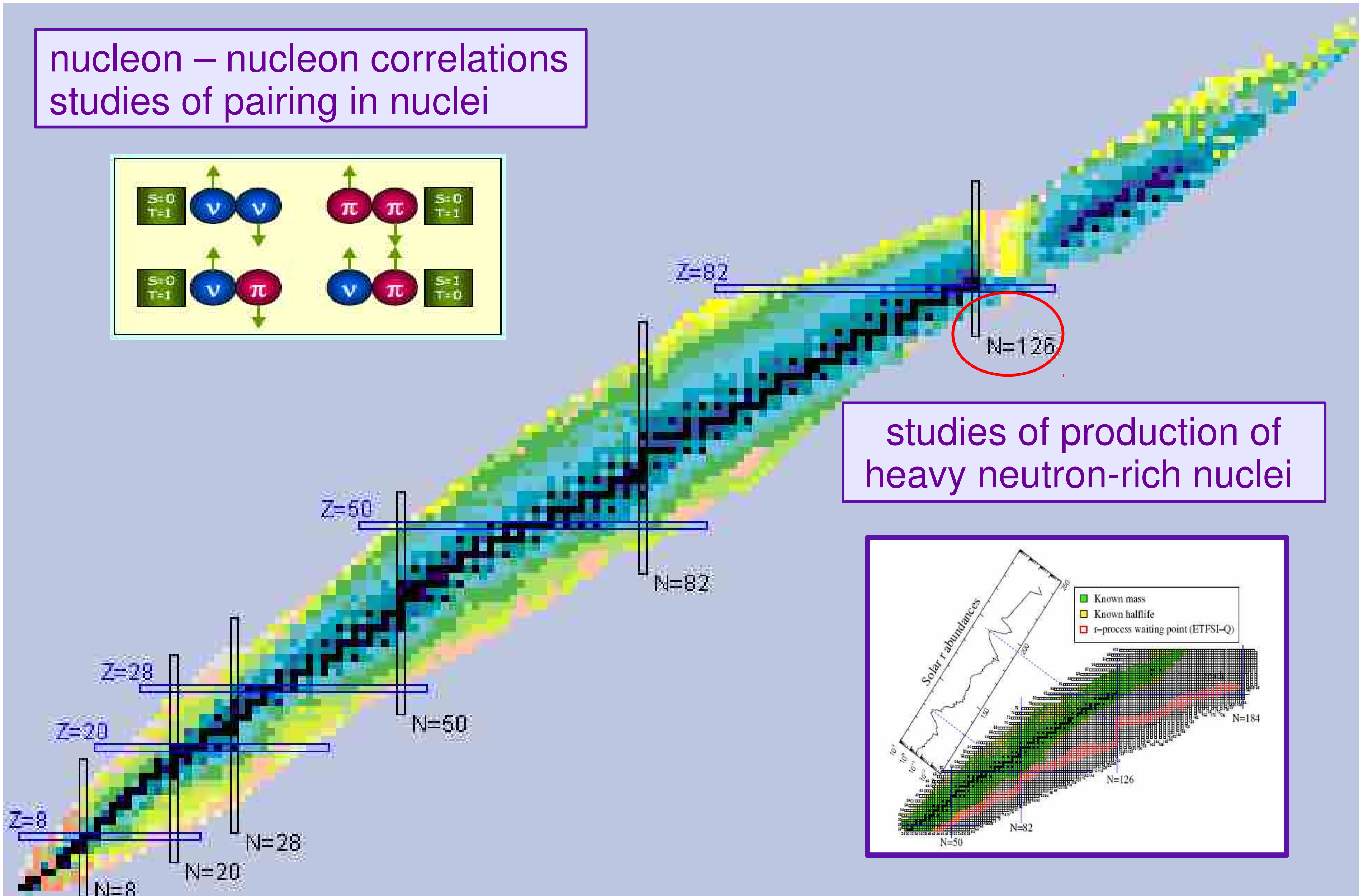

Probing nucleon-nucleon correlations in transfer reactions

The pairing interaction induces particle-particle correlations that are essential in defining the properties of finite quantum many body systems in their ground and neighboring states. These structure properties may influence in a significant way the evolution of the collision of two nuclei.

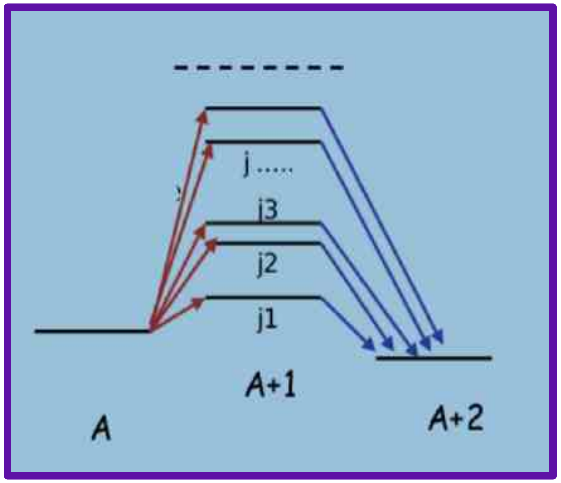

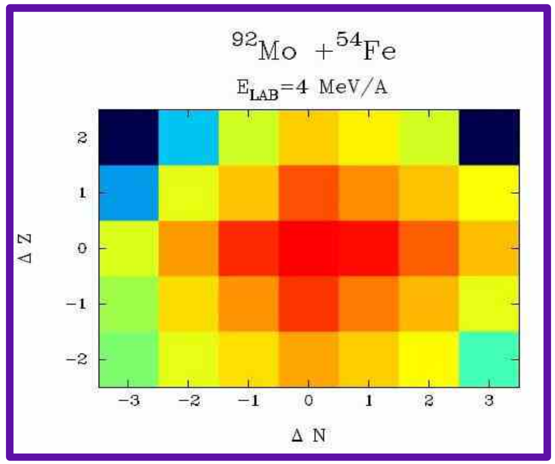

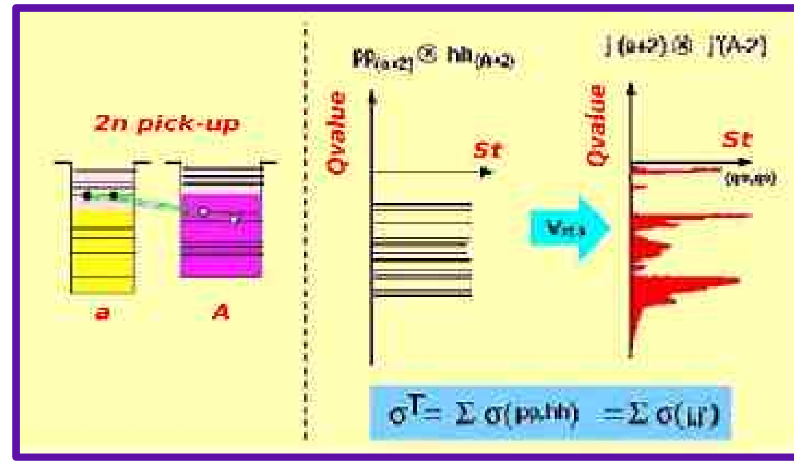

Heavy ion transfer reactions:

Advantages: test of correlation properties in transfer processes via simultaneous comparison of ±n and ±p, and ±nn/±pp/±np pairs; transfer of “many” pairs
HI drawbacks: limited A,Z, energy resolutions (two-nucleon transfer → redistribution of the strength around single particle states)

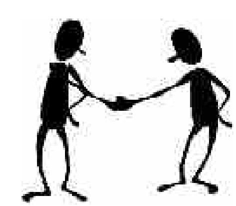

Nucleon-nucleon correlations studied with PRISMA

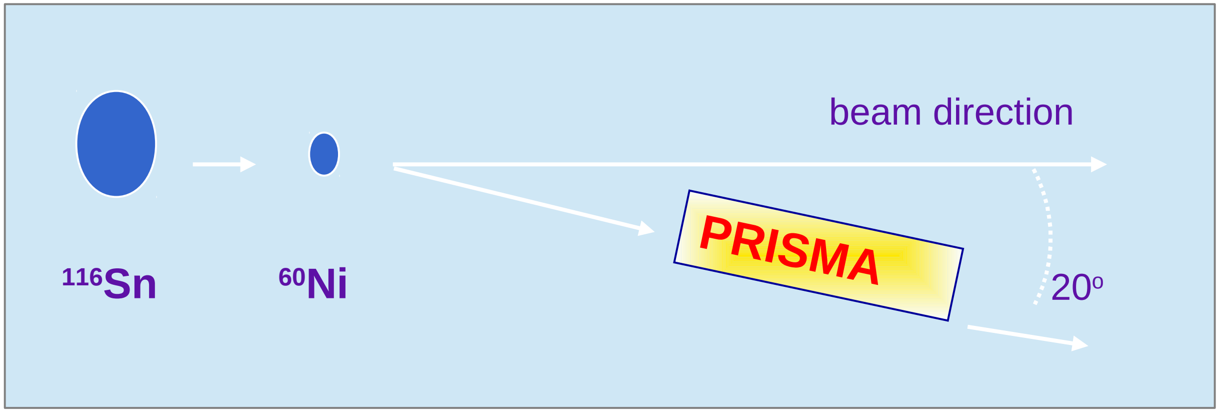

^{116}Sn+^{60}Ni, inverse kinematic, excitation function (detection of (lighter) target-like fragment in PRISMA:

E_{beam} = 500 MeV – 410 MeV

(D ~ 12.3 to 15.0 fm)

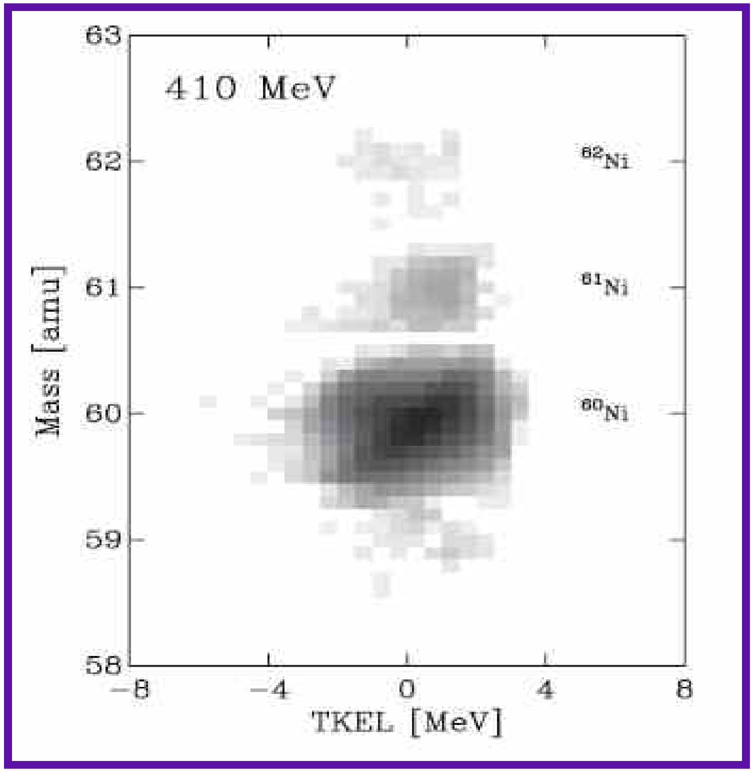

^{96}Zr+^{40}Ca, ^{116}Sn+^{60}Ni, ^{92}Mo+^{54}Fe, ^{206}Pb+^{116}Sn direct + inverse kinematic, PRISMA and PRISMA+CLARA/AGATA/LaBr (7 experiments)

^{96}Zr+^{40}Ca: S. Szilner et al., Phys. Rev. C 76 (2007) 024604; L. Corradi et al., Phys. Rev. C 84 (2011) 034603

^{116}Sn+^{60}Ni: D. Montanari et al., Phys. Rev. Lett. 113 (2014) 052501; D. Montanari et al., Phys. Rev. C 93 (2016) 054623

Measurements below Coulomb barrier

$^{116}Sn(^{60}Ni,^{62}Ni)$
$Q_{gs} = +1.3$ MeV

A smooth transition between QE and DIC

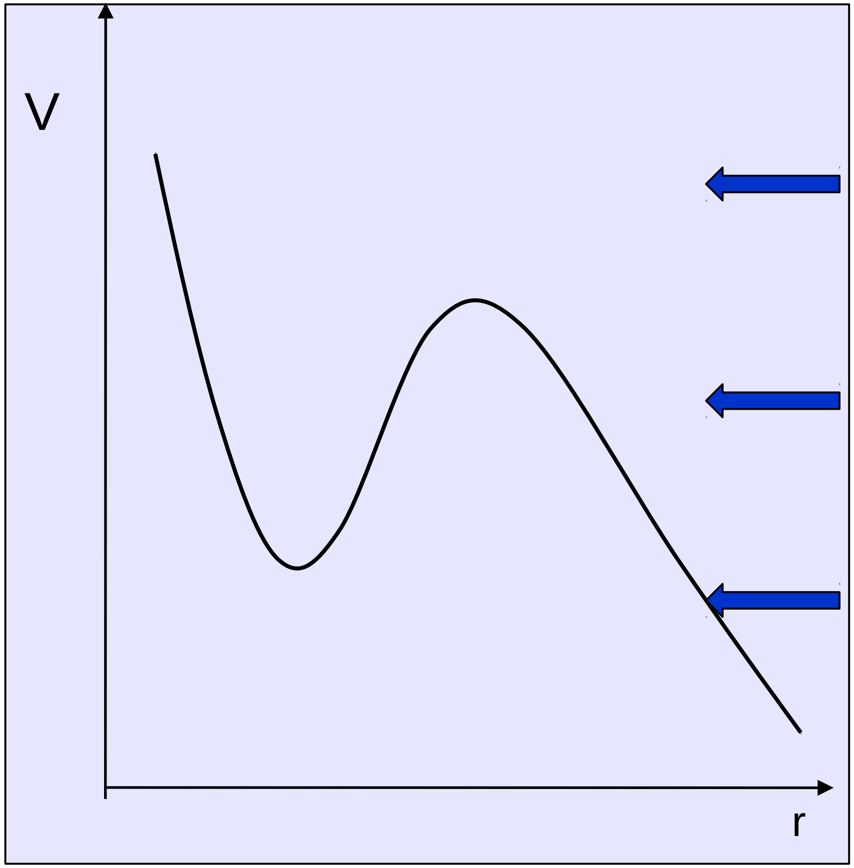

$E > E_b$

$E \sim E_b$

$E < E_b$

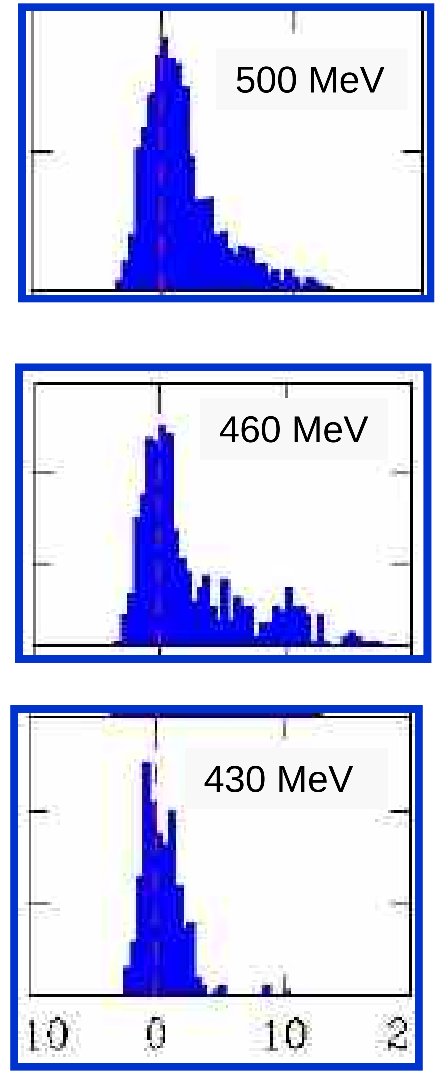

Below the barrier Q-values gets very narrow and without DIC components:
1) $E > E_b$ large number of open channels, DIC components / evaporation effects
2) $E < E_b$ narrow Q-value distributions (concentrated at "one state")

D. Montanari et. al., PRL 113 (2014) 052501

$^{116}Sn+^{60}Ni$: neutron pair transfer far below the Coulomb barrier

Transfer strength very close to the g.s. to g.s. transitions

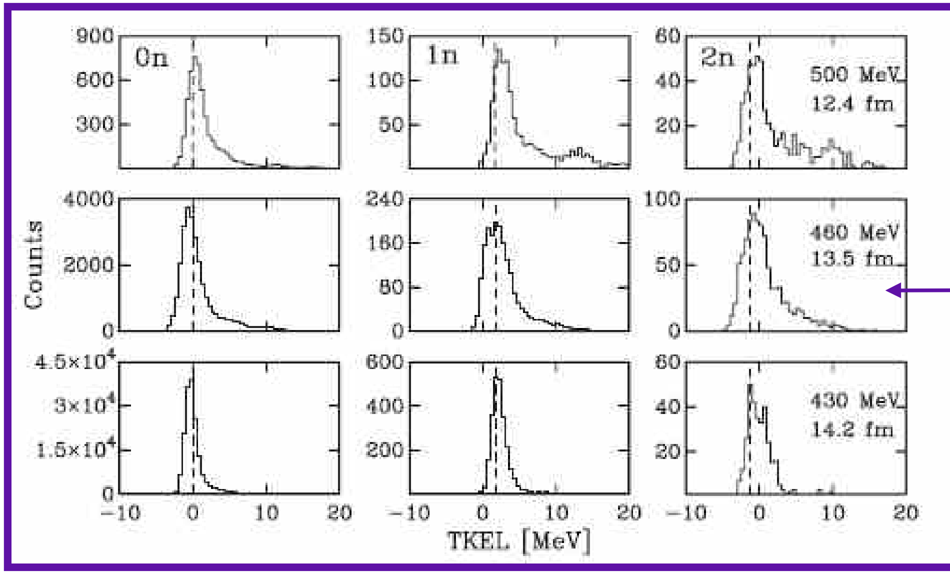

Coulomb barrier

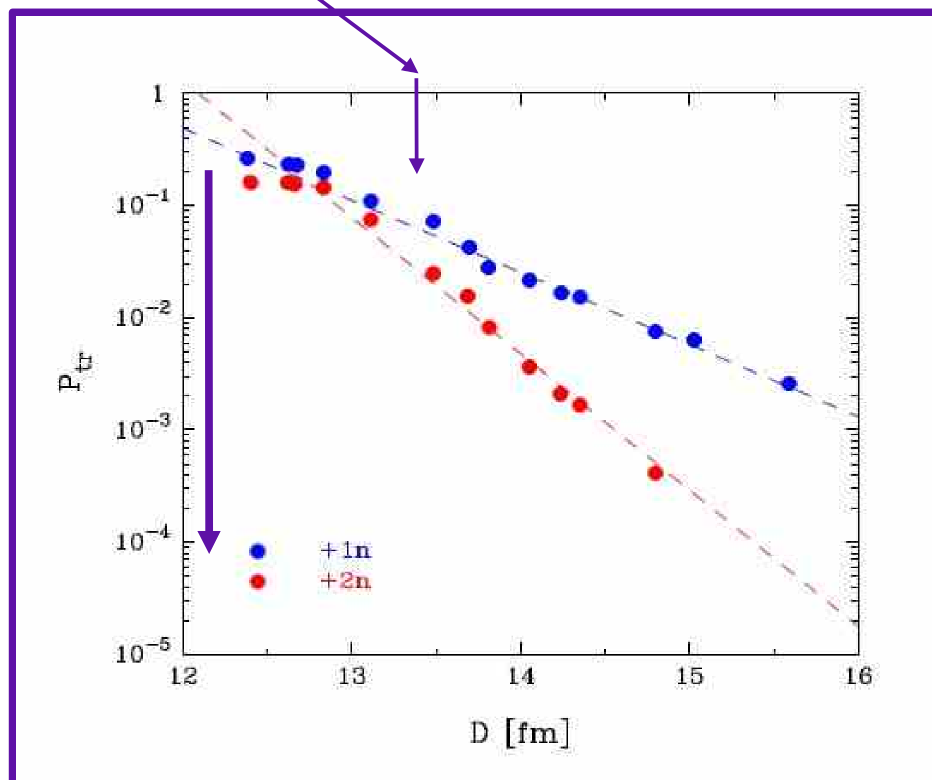

D. Montanari et. al., Phys. Rev. Lett. 113 (2014) 052501

$$P_{tr} = \frac{d\sigma_{tr}}{d\sigma_{\mathrm{Ruth}}}$$

$$D = \frac{Z_a Z_A e^2}{2E_{\mathrm{c.m.}}}\left(1 + \frac{1}{\sin(\theta_{\mathrm{c.m.}}/2)}\right)$$

^{60}Ni+^{116}Sn, ^{40}Ca+^{96}Zr, ^{54}Fe+^{92}Mo: fragment – gamma measurements (PRISMA+CLARA/AGATA/LaBr)

^{60}Ni+^{116}Sn: angular distributions measurement in "direct" kinematic:

E_{beam} = 245 MeV at 70^0 (D ~ 14.5 fm)

$$D = \frac{Z_a Z_A e^2}{2E_{c.m.}}\left(1 + \frac{1}{\sin(\theta_{c.m.}/2)}\right)$$

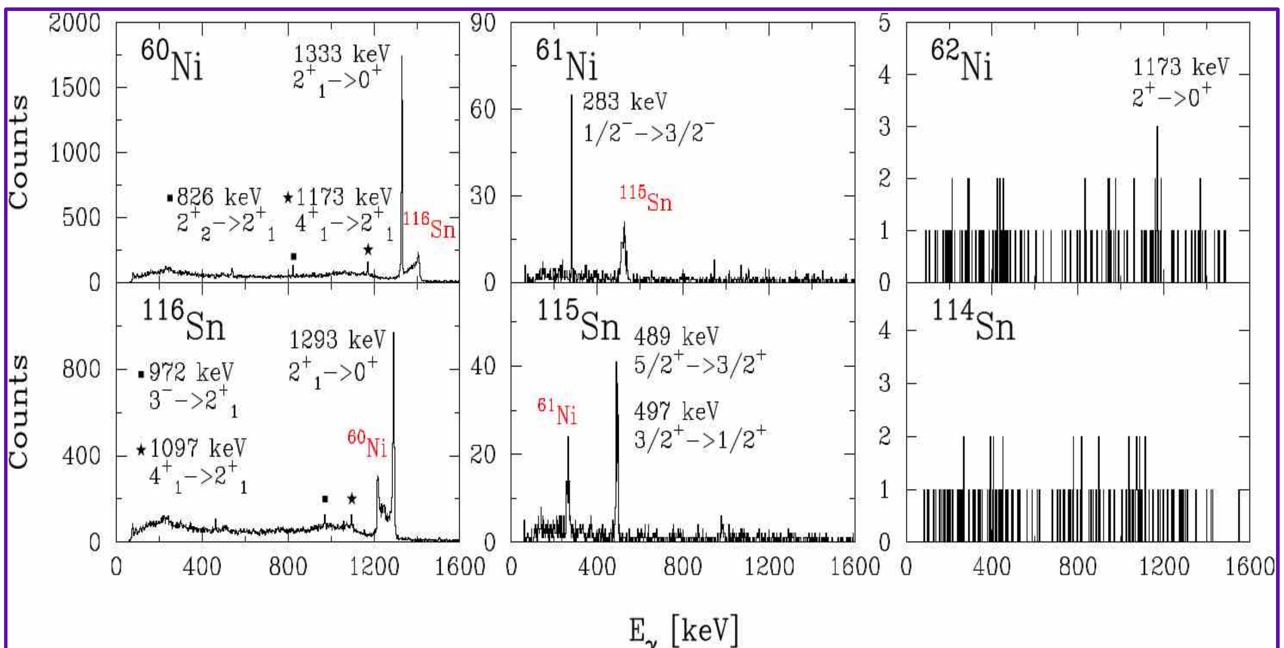

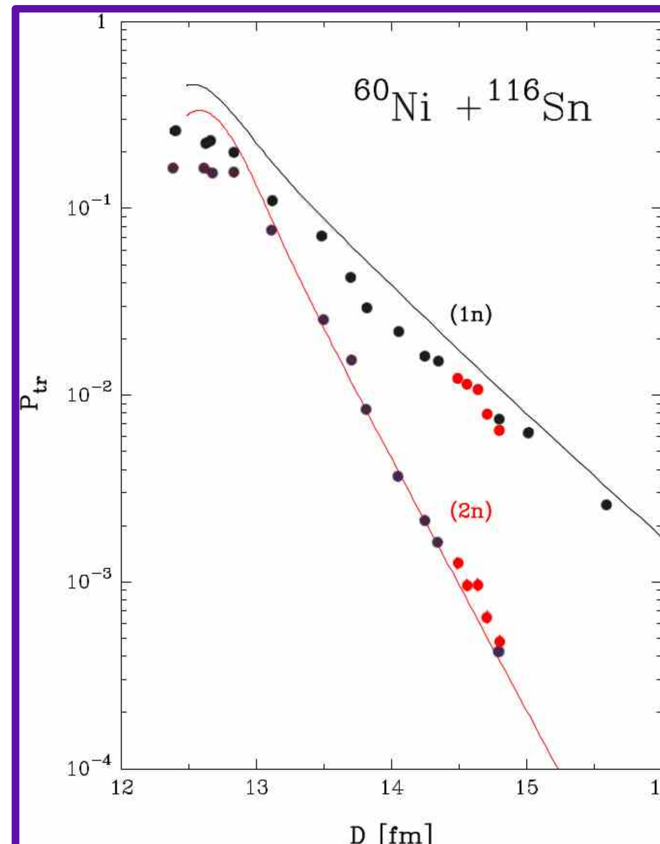

^{60}Ni+^{116}Sn, ^{40}Ca+^{96}Zr, ^{54}Fe+^{92}Mo: fragment – gamma measurements (PRISMA+CLARA/AGATA/LaBr)

The strengths (normalized to $2^+ \rightarrow 0^+$ in ^{60}Ni) of the most important transitions are compared with a reaction code (DWBA, CC, SF) $\rightarrow$ a direct check on the one-particle form factors (1n), and of the potential
(2n): $\sigma_{g.s} = \sigma_{tot} - \sigma_{exc}$ $\rightarrow$ the transitions to the excited states contribute to the total strength: <24%, **dominant population of the ground states**

$$D = \frac{Z_a Z_A e^2}{2E_{c.m.}}\left(1 + \frac{1}{\sin(\theta_{c.m.}/2)}\right)$$

	Experiment	Theory
^{116}Sn(2^+)	0.792 ± 0.160	0.720
^{116}Sn(4^+_1)	0.042 ± 0.011	0.056
^{60}Ni(4^+_1)	0.060 ± 0.013	0.11
^{115}Sn($5/2^+$)	0.018 ± 0.003	0.037
^{61}Ni($1/2^-$)	0.014 ± 0.003	0.033
^{62}Ni(2^+)	< 0.00145	-

E_γ [keV]

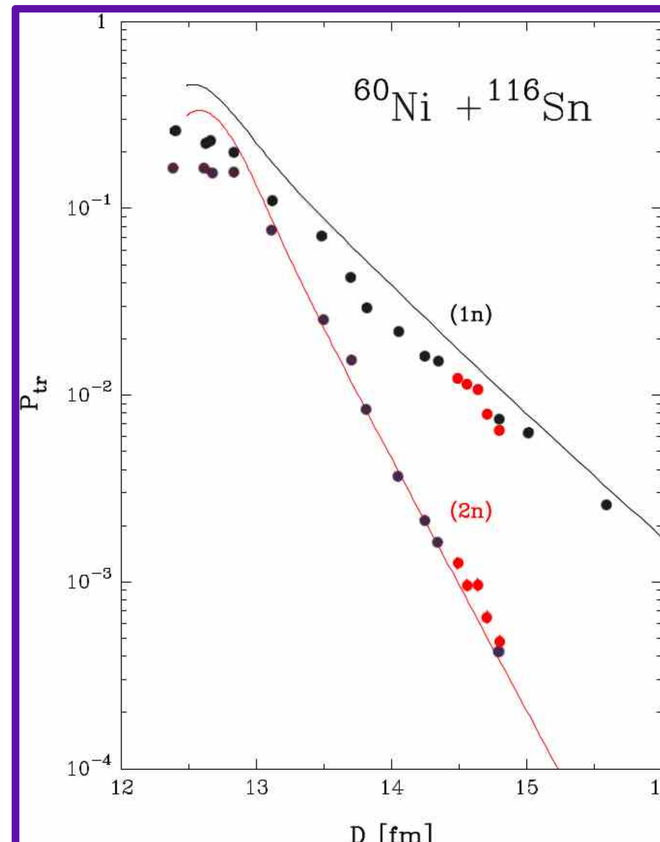

^{116}Sn+^{60}Ni: two particle transfer (semiclassical theory, microscopic calculations, 2nd order Born app.)

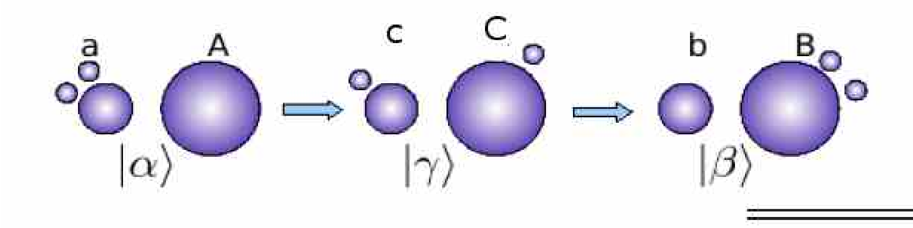

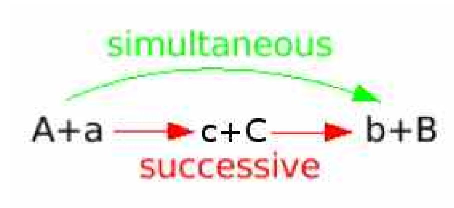

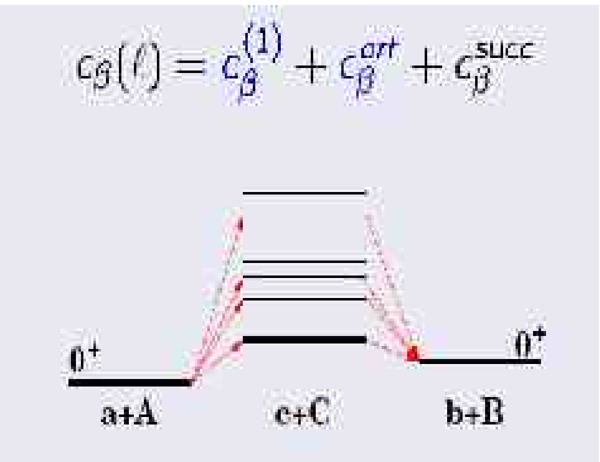

	nlj
^{116}Sn	$1g_{9/2}$
	$2d_{5/2}$
	$1g_{7/2}$
	$3s_{1/2}$
	$2d_{3/2}$
	$1h_{11/2}$
	$2f_{7/2}$
	$3p_{3/2}$
^{60}Ni	$2p_{3/2}$
	$2p_{1/2}$
	$1f_{5/2}$
	$1g_{9/2}$

3 terms : simultaneous, orthogonal and successive

only the successive term contributes to the transfer amplitude (simultaneous component is canceled out by the nonorthogonality correction)

Only 0+ to 0+ transitions are included (BCS).

$$(c_\beta)_{\rm succ} = \frac{1}{\hbar^2} \sum_{a_1, a_1'} B^{(A)}(a_1 a_1; 0) B^{(a)}(a_1' a_1'; 0) 2 \frac{(-1)^{j_1 + j_1'}}{\sqrt{(2j_1+1)}\sqrt{(2j_1'+1)}} \sum_{m_1 m_1'} (-1)^{m_1 + m_1'}$$
$$\times \int_{-\infty}^{+\infty} dt\, f_{m_1 m_1'}(\mathcal{R}) e^{i[(E_\beta - E_\gamma)t + \delta_{\beta\gamma}(t) + \hbar(m_1' - m_1)\Phi(t)]/\hbar}$$
$$\times \int_{-\infty}^{t} dt\, f_{-m_1 - m_1'}(\mathcal{R}) e^{i[(E_\gamma - E_\alpha)t + \delta_{\gamma\alpha}(t) - \hbar(m_1' - m_1)\Phi(t)]/\hbar}.$$

$^{60}Ni+^{116}Sn$: neutron pair transfer far below the Coulomb barrier

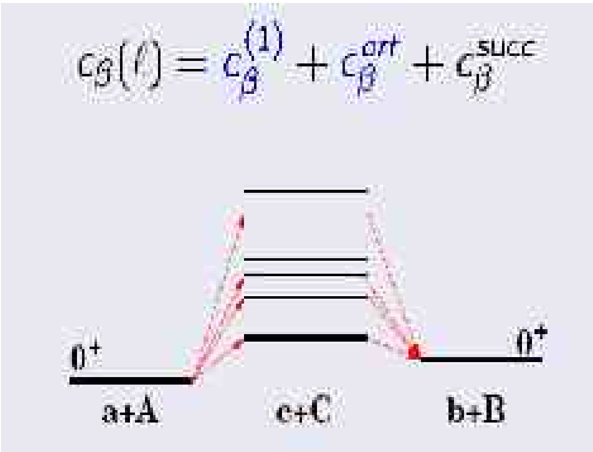

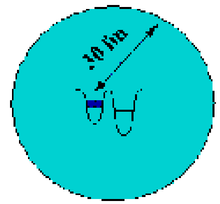

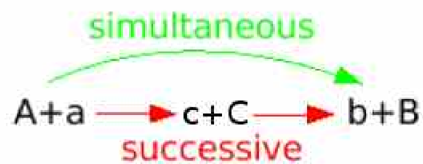

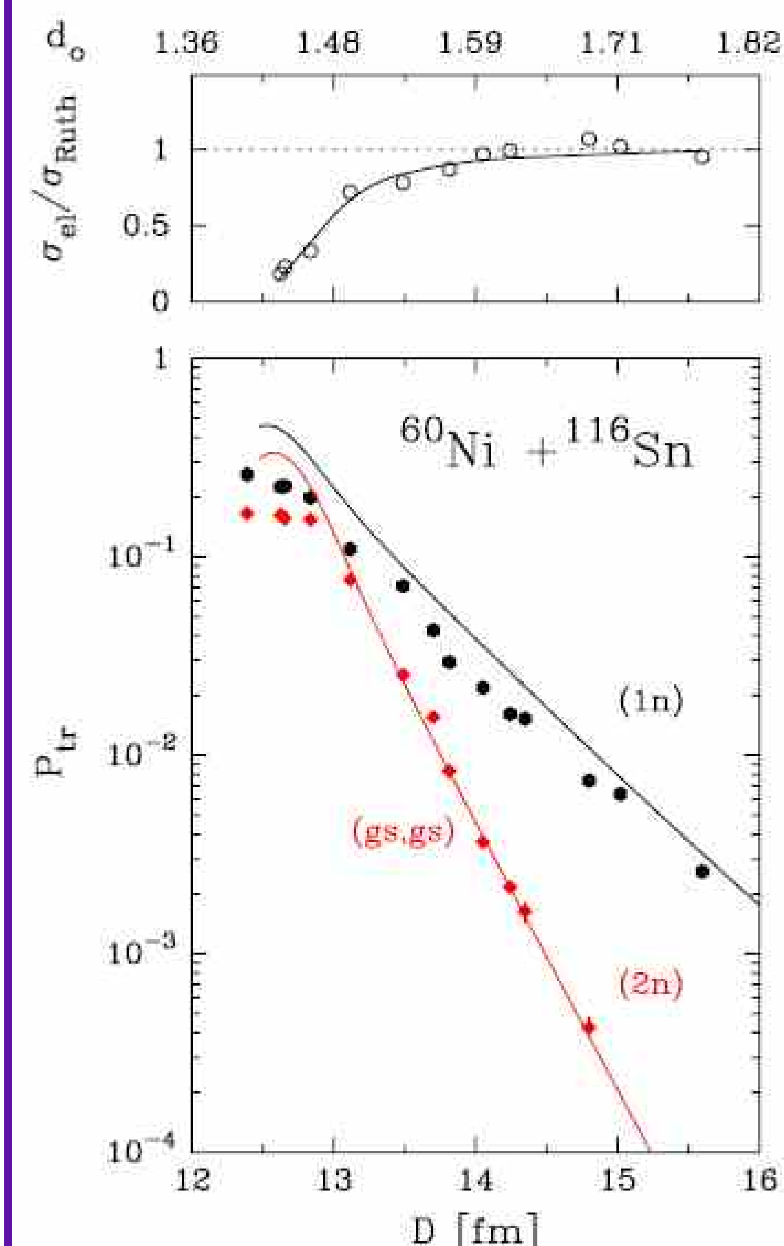

The experimental transfer probabilities are well reproduced, in absolute values and in slope by microscopic calculations which incorporate nucleon-nucleon correlations:

✓ a consistent description of (1n) and (2n) channels

✓ the formalism for (2n) incorporates the contribution from both the simultaneous and successive terms (only the ground-to-ground-state transition has been calculated)

✓character of pairing correlations manifests itself equally well in simultaneous and in successive transfers due to the correlation length

The Josephson effect in nuclear physics

For distances of closest approach compatible with the correlation length ξ the two nucleons behave like (quasi)bosons

$$\xi = \frac{\hbar v_F}{\pi \Delta} \approx 13.5 \text{ fm}$$

$$P_2 \approx P_1$$

At large distances of closest approach the Cooper pairs loose their (quasi)boson character and acquire a quasiparticle nature. One has a simple tunnelling of nucleons through the inner barrier

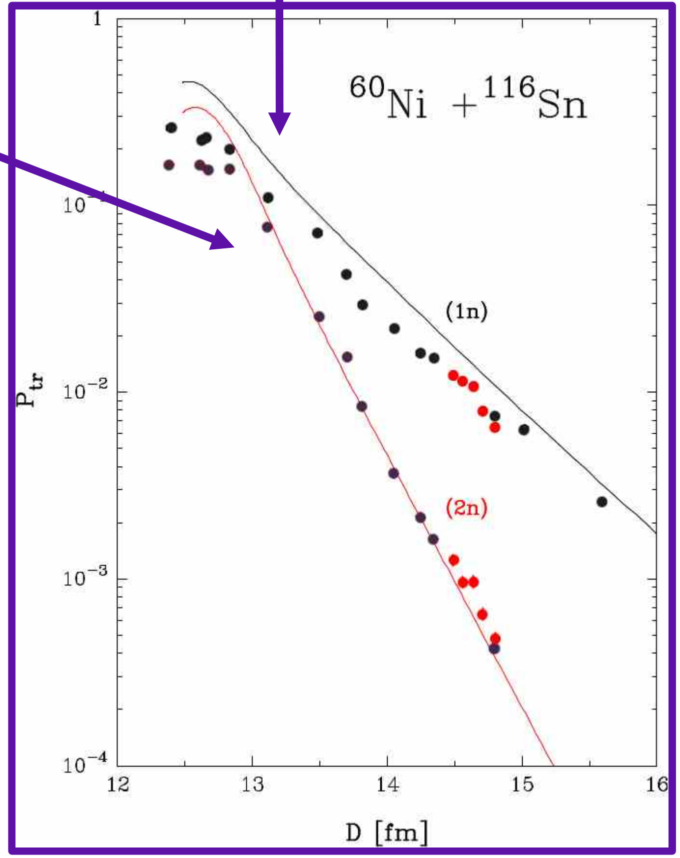

G. Potel, F. Barranco, E. Vigezzi, and R. A. Broglia

Phys. Rev. C 103 (2021) L021601

$^{206}Pb+^{118}Sn$: complex reaction mechanism

E(^{206}Pb)=1200 MeV

θ_{lab}=25^{o}

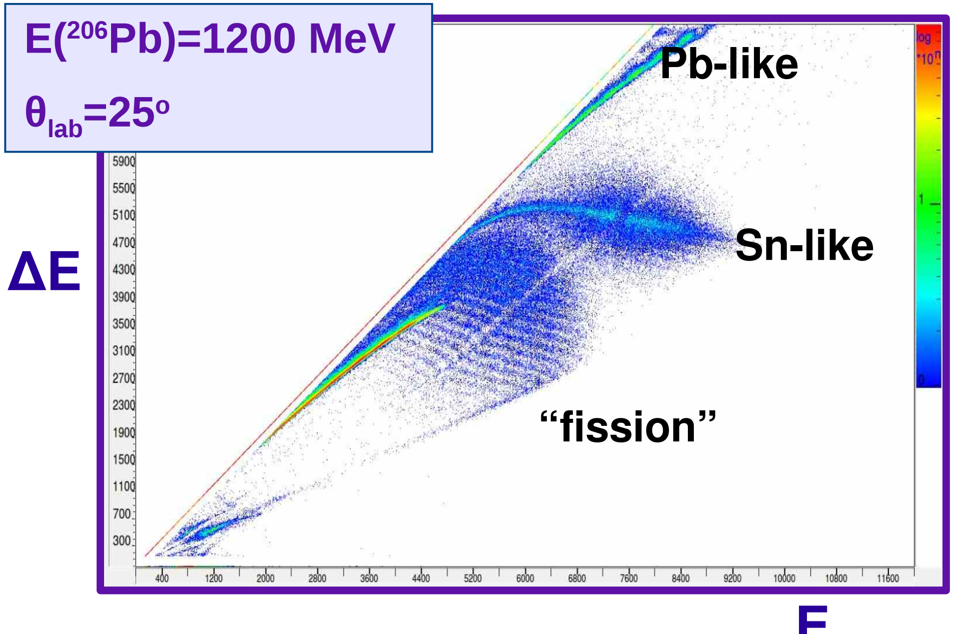

E(^{206}Pb)=1200 MeV

θ_{lab}=35^{o}

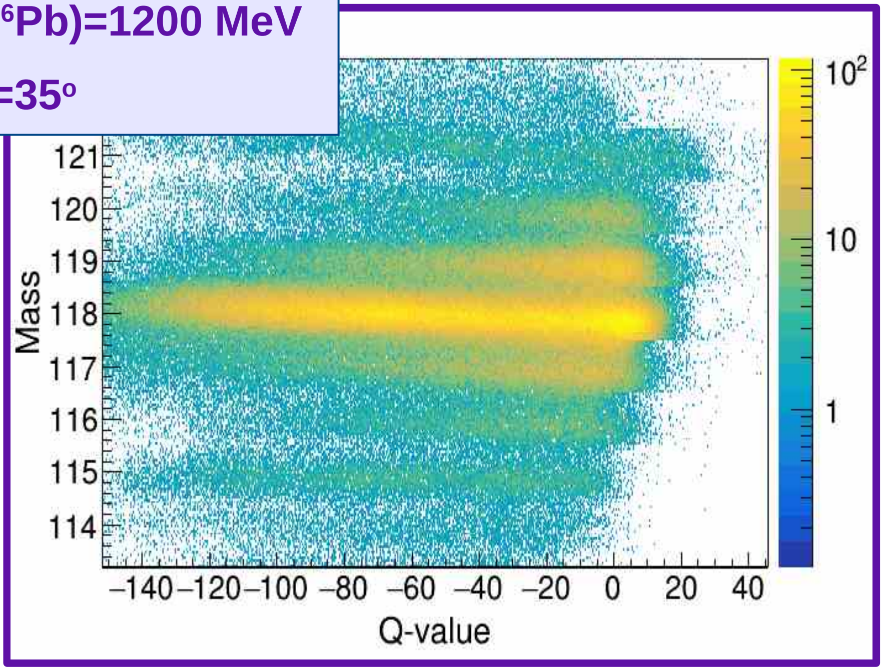

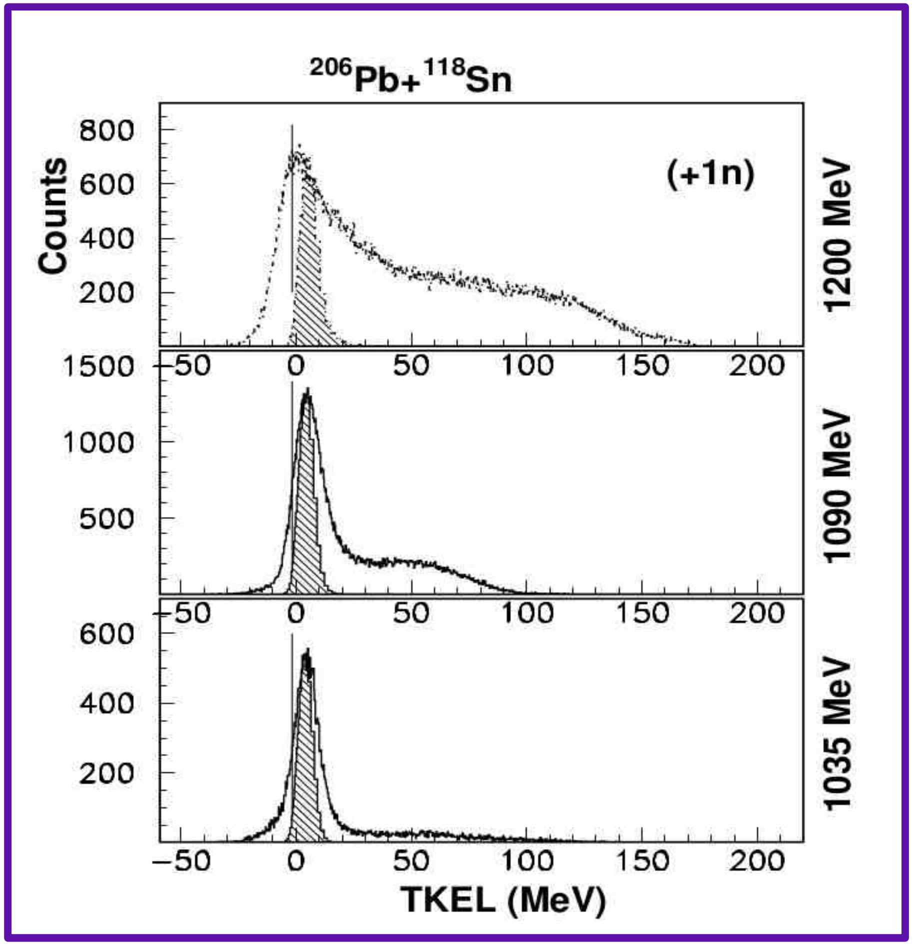

INFN – LNL, PRISMA spectrometer, 2018, L. Corradi, S. Szilner, J. Diklić, Ph.D. Thesis

Nucleon transfer: exp. vs microscopic calculatons

$^{96}Zr+^{40}Ca$ ("closed shell")

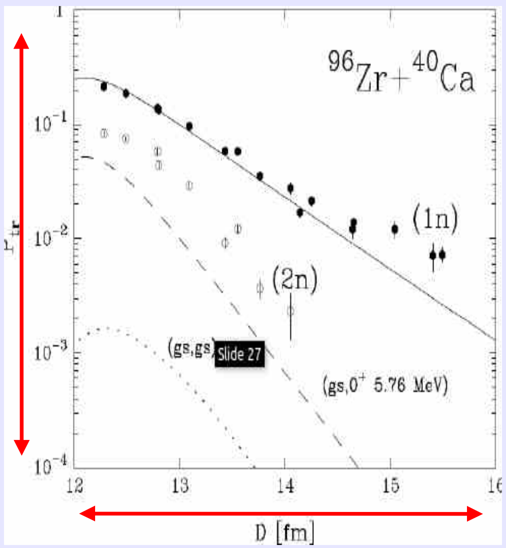

L. Corradi et al.,
PRC 84 (2011) 034603

$^{116}Sn+^{60}Ni$ ("superfluid")

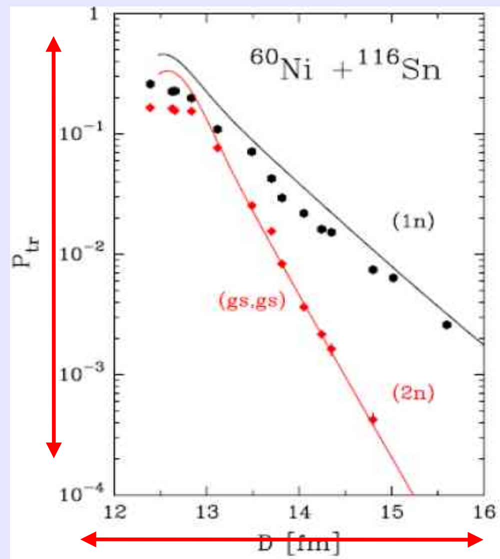

D. Montanari et al.,
PRL 113 (2014) 052501
PRC 93 (2016) 054623

$^{206}Pb+^{118}Sn$ ("heavy")

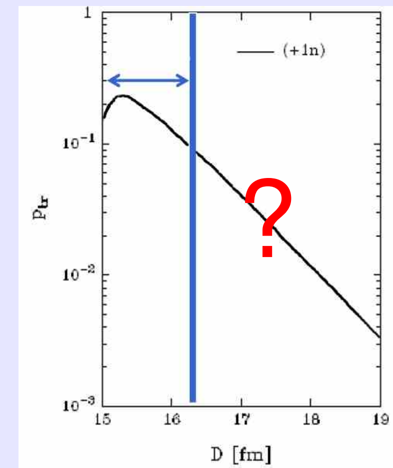

$^{132}Sn+^{40}Ca,^{64}Ni,^{208}Pb$ ("neutron rich")

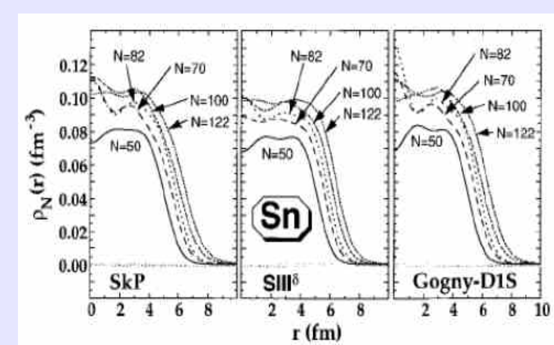

Nucleon transfer: exp. vs microscopic calculatons

^{96}Zr+^{40}Ca ("closed shell")

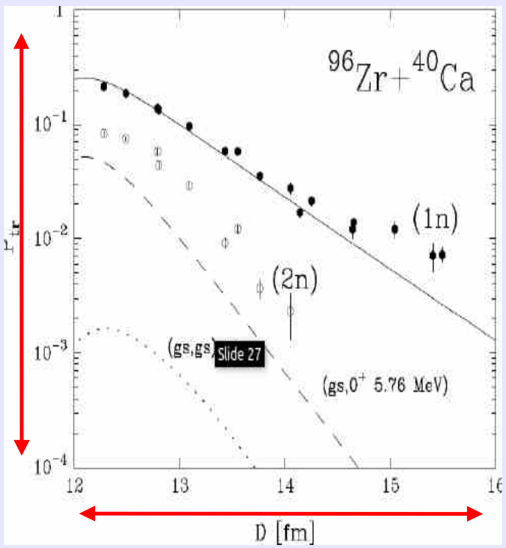

^{116}Sn+^{60}Ni ("superfluid")

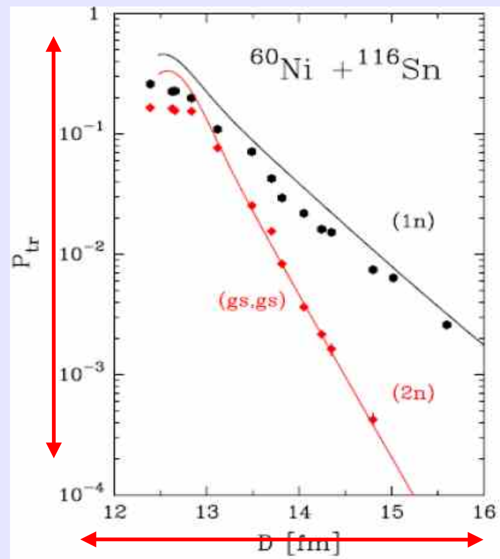

^{206}Pb+^{118}Sn ("heavy")

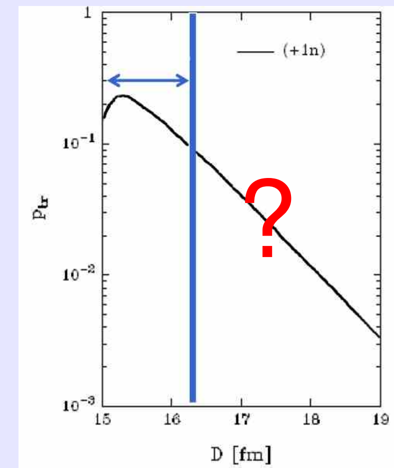

^{132}Sn+^{40}Ca,^{64}Ni,^{208}Pb ("neutron rich")

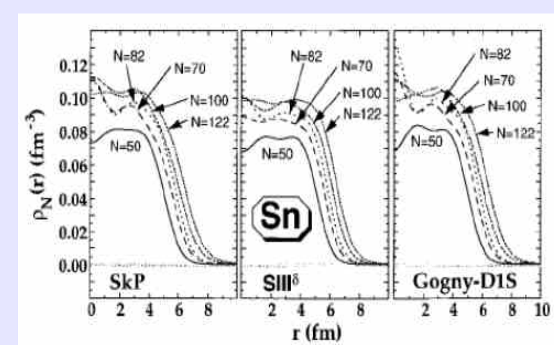

informations about correlations are extracted when experimental absolute cross sections are compared with a microscopic theory which beside correlations includes also the coupling between relative motion (reaction) and intrinsic motion (structure).

Synthesis of heavy neutron rich nuclei in labs

Fusion by using neutron-rich radioactive beams $\rightarrow$ the intensity of the beams rather small (accelerators)

Neutron capture reaction $\rightarrow$ the intensity of the neutron beams is small (reactors)

relativistic energies : fragmentation reactions
energies close to the Coulomb barrier : multinucleon transfer reactions
$\rightarrow$ cross sections ~ μb – nb
$\rightarrow$ detection systems: large solid angle, large efficiency, large selectivity...

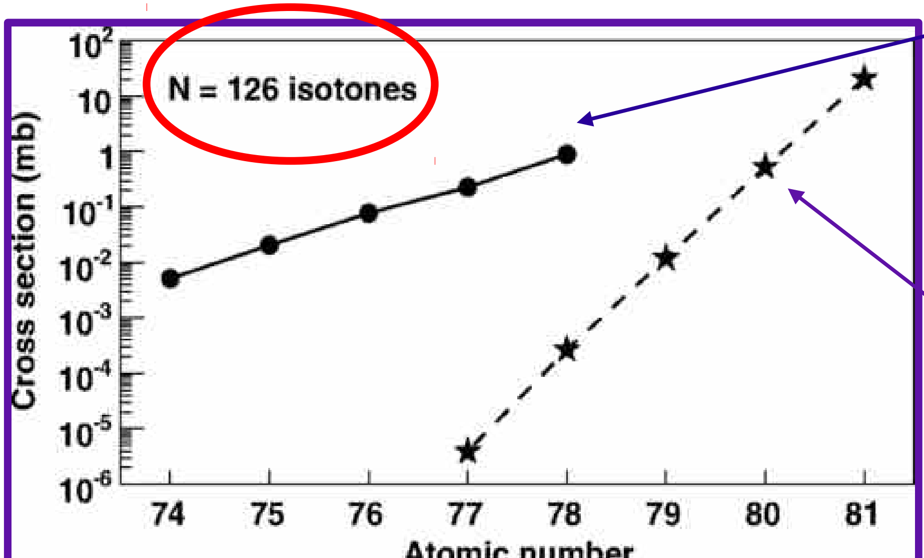

multinucleon transfer reactions:
$^{136}Xe + ^{198}Pt$ @ E_{lab}= 8 MeV/A

fragmentation reactions:
$^{208}Pb + ^{9}Be$ @ E_{lab}= 1 GeV/A

Y. Watanabe et al, Phys. Rev. Lett. 115 (2015) 172503, T. Kurtukian-Nieto et al., Phys. Rev. C 89 (2014) 024616.

Multinucleon transfer reactions

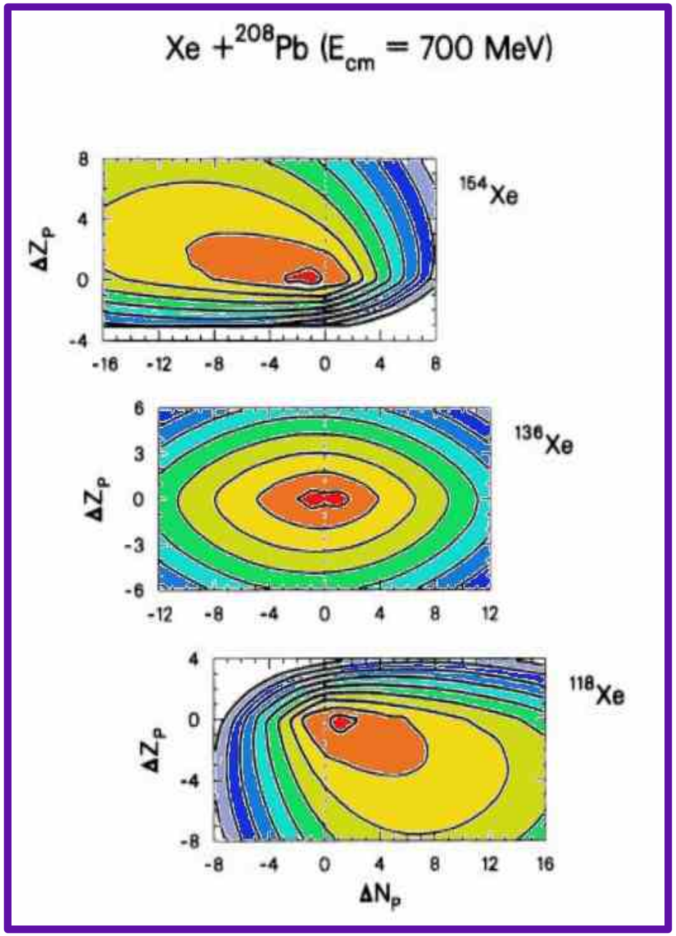

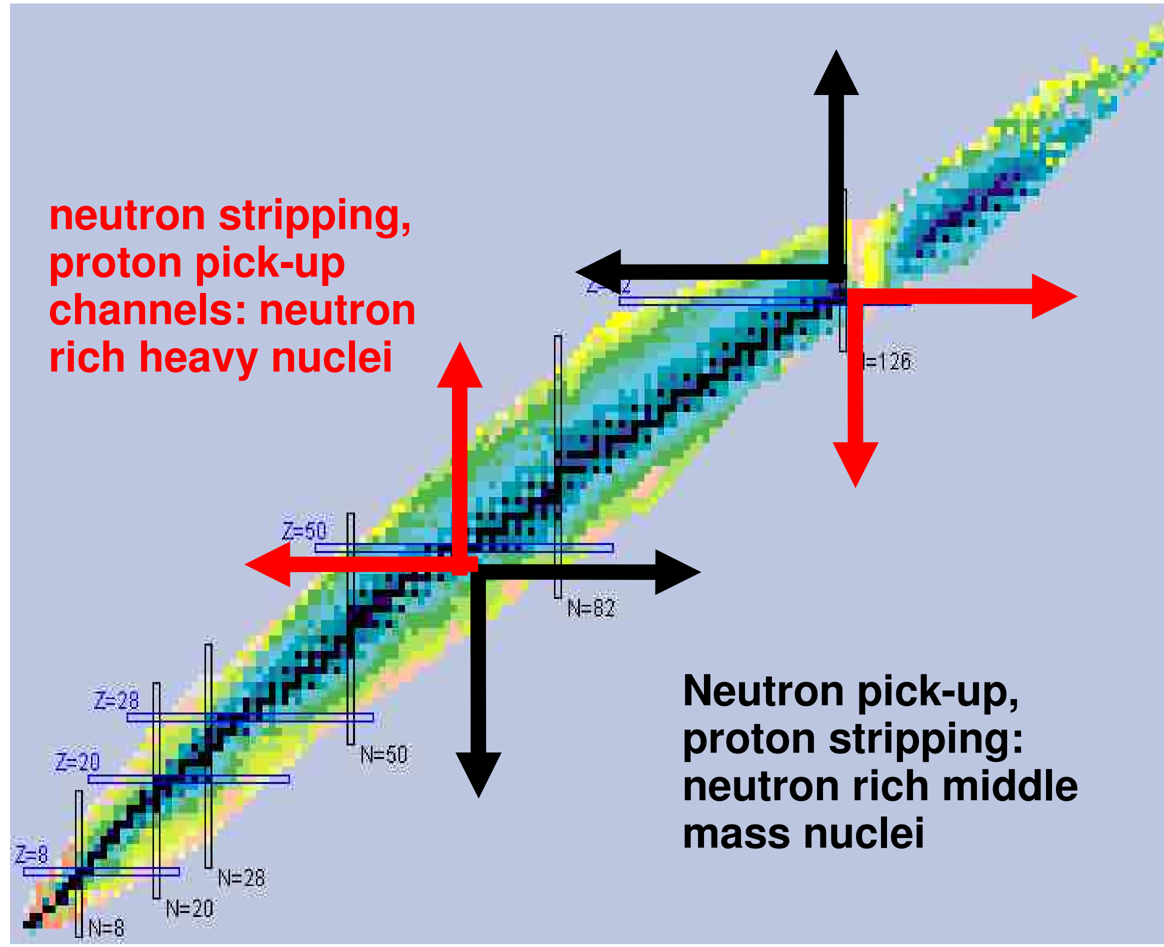

Xe (Z=54)
^{118}Xe ($T_{1/2}$ = 4 min)
^{136}Xe ("the last" stable)
^{154}Xe (no information)

TH: C.H. Dasso, G. Pollarolo and A. Winther, Phys. Rev. Lett. 73 (1994) 1907.
EXP: L. Corradi, G. Pollarolo, S. Szilner, J. Phys. G 36 (2009) 113101 (Special Topic)

$^{40}Ar+^{208}Pb$, $^{40}Ca+^{208}Pb$, and $^{58}Ni+^{208}Pb$

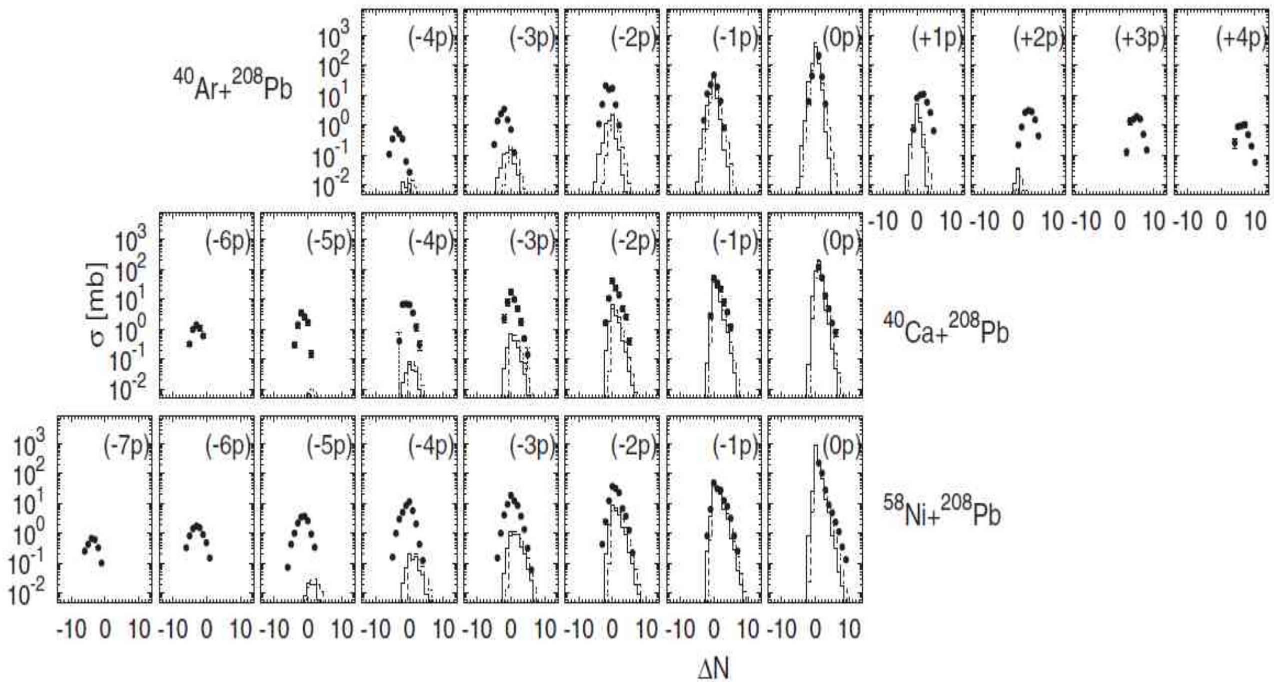

Above the barrier:
→ many open channels, transfer of 5-10 protons and neutrons governed by optimum Q-value
→ large TKEL, onset of DIC components
→ secondary processes: evaporation, transfer induced fission

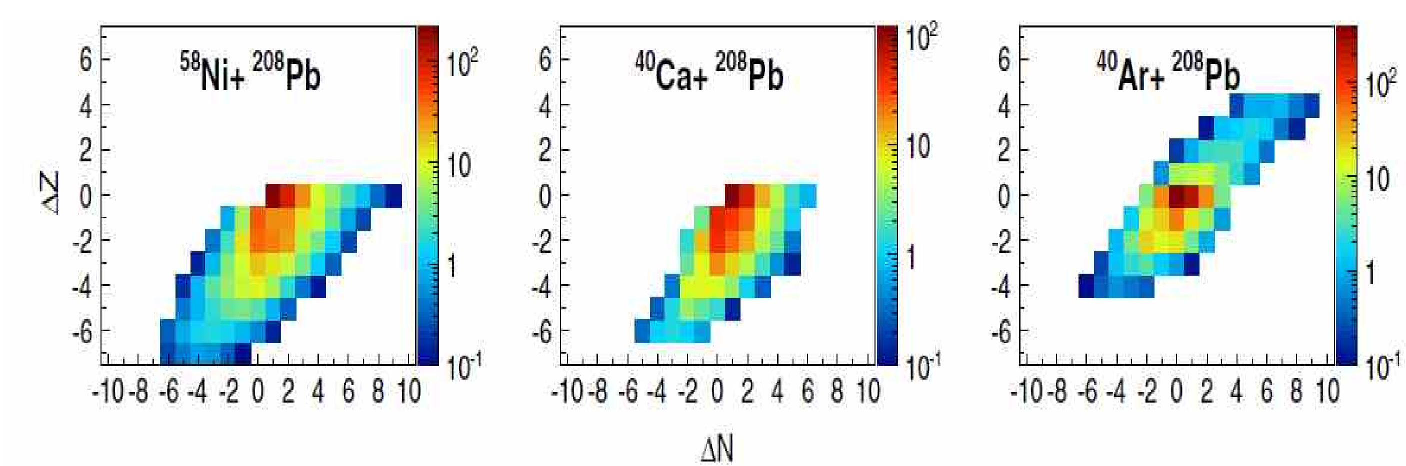

Wilczynski plots

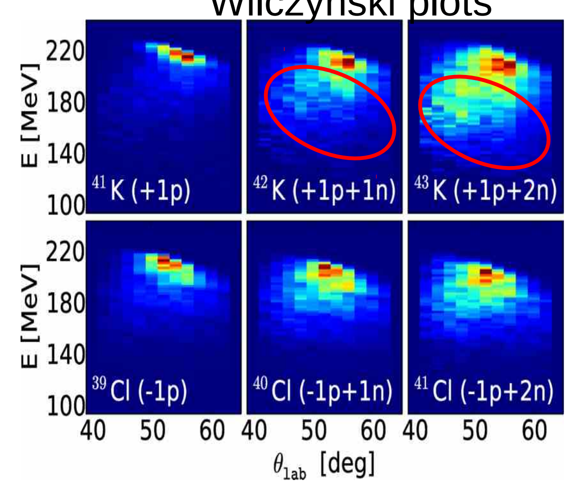

$^{40}Ar+^{208}Pb$

T. Mijatovic et al., Phys. Rev. C 94 (2016) 064616

$^{40}Ar+^{208}Pb$

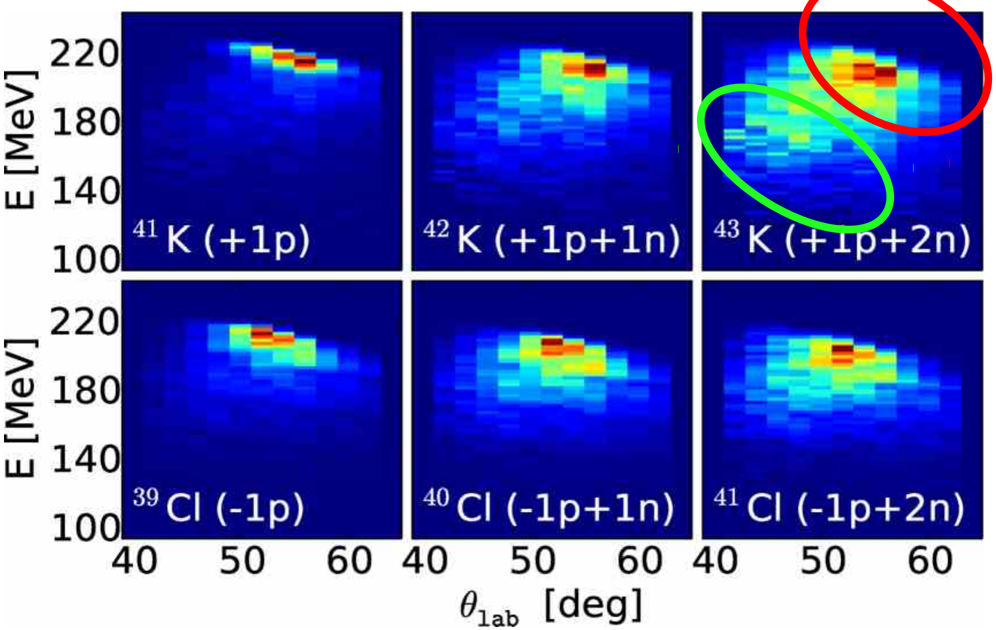

Wilczynski plots

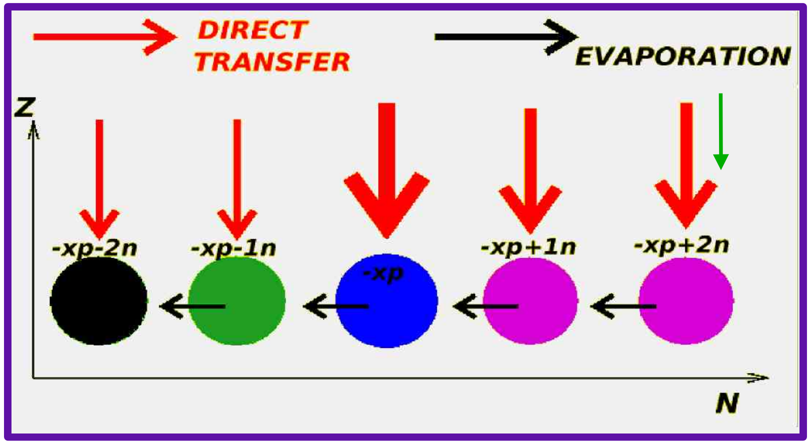

- ✓Reaction develops from quasi-elastic to deep inelastic
- ✓Secondary processes are important (fission, evaporation of neutrons may strongly modify the final cross sections) → survival probability of the heavy binary partner

+2n channel: $^{40}Ar+^{208}Pb \rightarrow {}^{42}Ar+^{206}Pb$

~90% of the yield corresponds to the true binary partner (^{206}Pb)

T. Mijatović et al., Phys. Rev. C 94 (2016) 064616

$^{40}Ar+^{208}Pb$

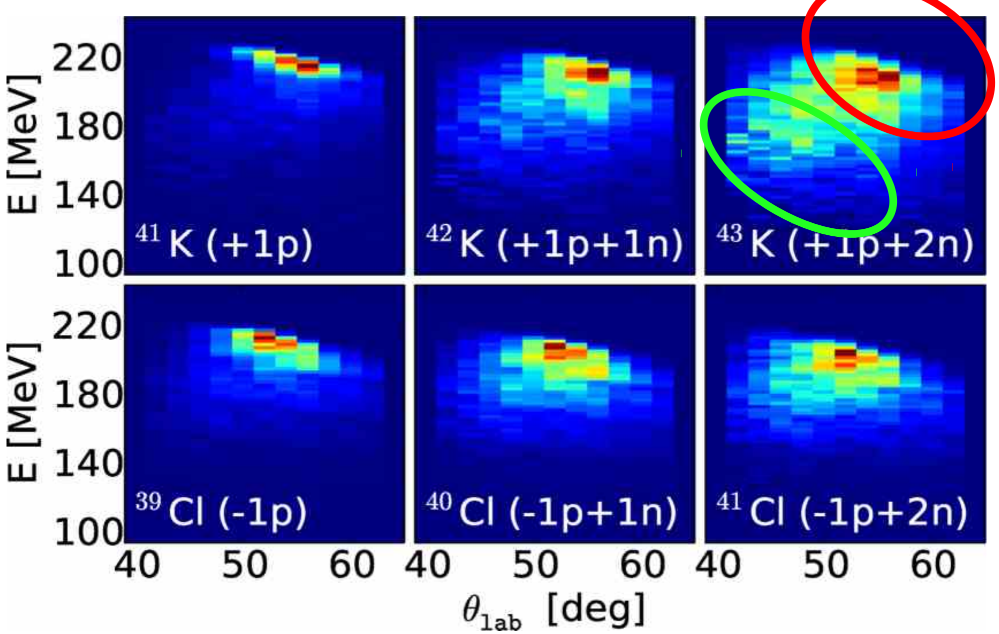

Wilczynski plots

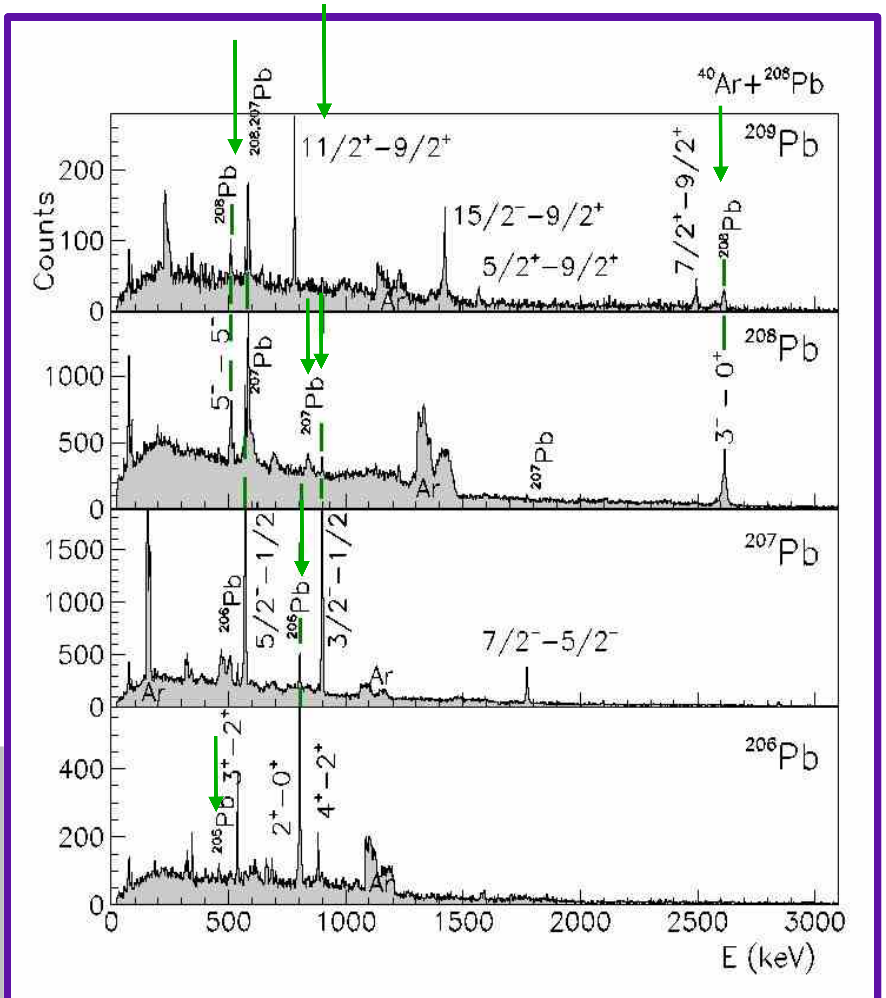

- Reaction develops from quasi-elastic to deep inelastic
- Secondary processes are important (fission, evaporation of neutrons may strongly modify the final cross sections) → survival probability of the heavy binary partner

+2n channel: $^{40}Ar+^{208}Pb$ → $^{42}Ar+^{206}Pb$

~90% of the yield corresponds to the true binary partner (^{206}Pb)

T. Mijatović et al., Phys. Rev. C 94 (2016) 064616

^{197}Au+^{130}Te: coincident detection of binary partners

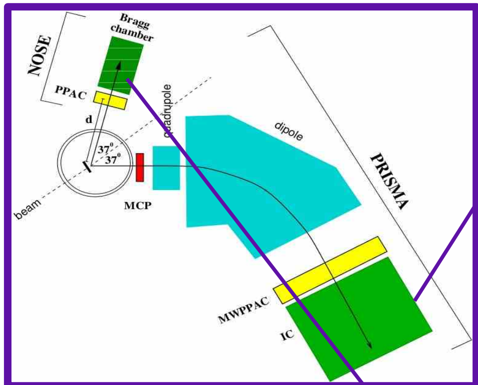

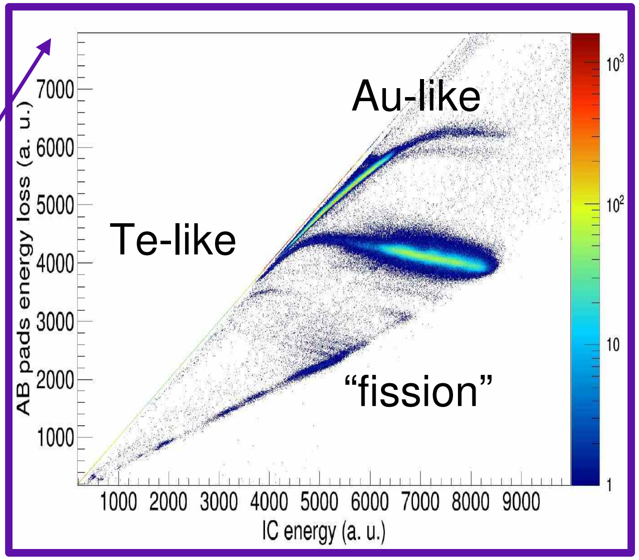

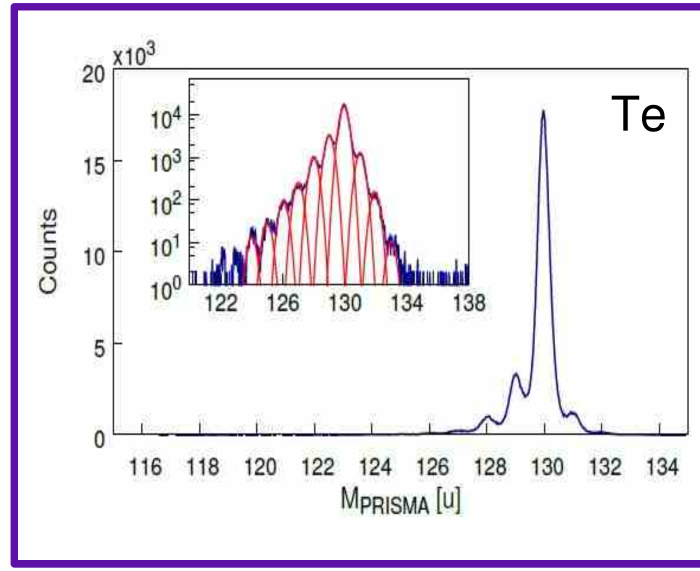

PRISMA

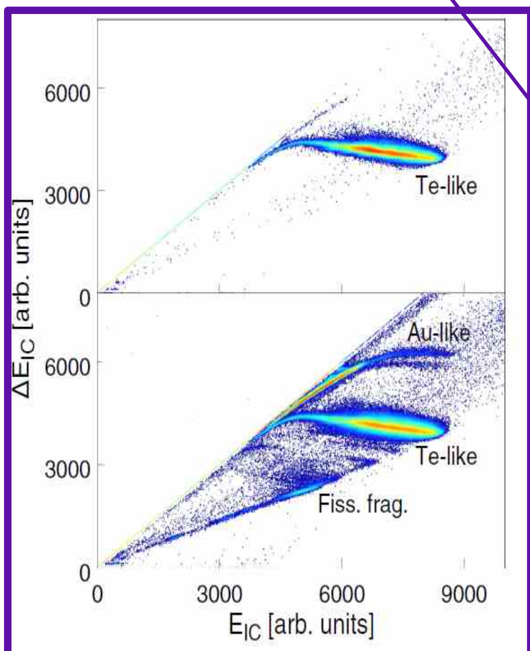

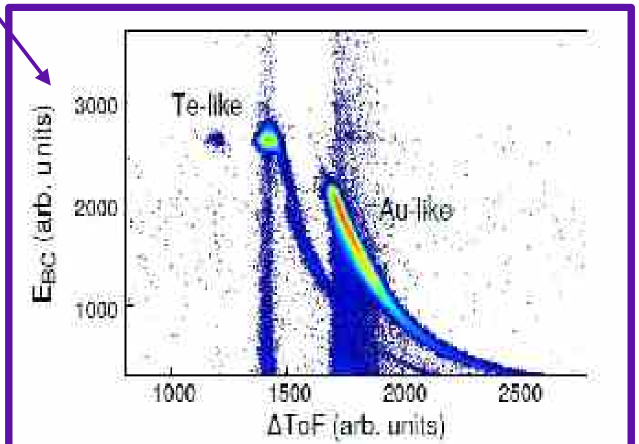

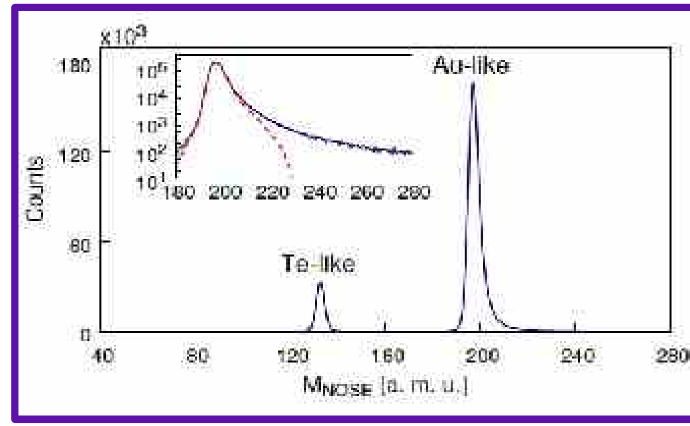

NOSE

F. Galtarossa et al., Phys. Rev. C 97 (2018) 054606
E. Fioretto et al. Nucl. Inst. and Meth. A 899 (2018) 73
A gas detection system for fragment identification in low-energy heavy-ion collisions

^{197}Au+^{130}Te

^{197}Au+^{130}Te: coincident detection of binary partenrs

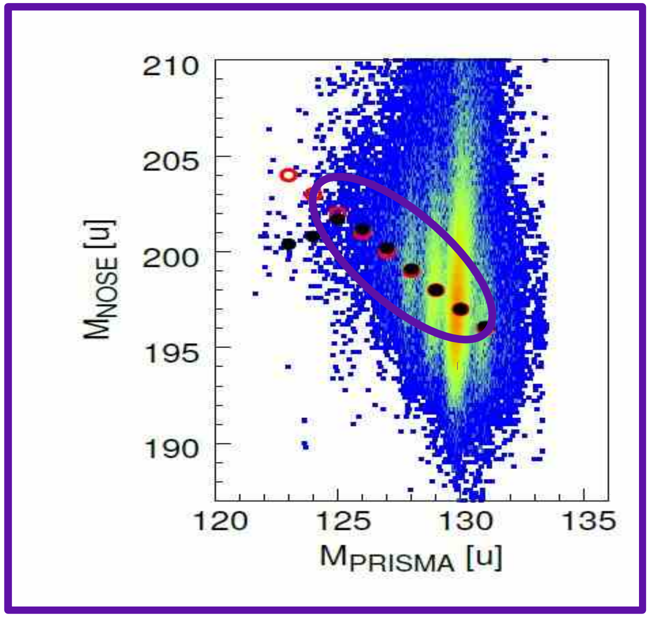

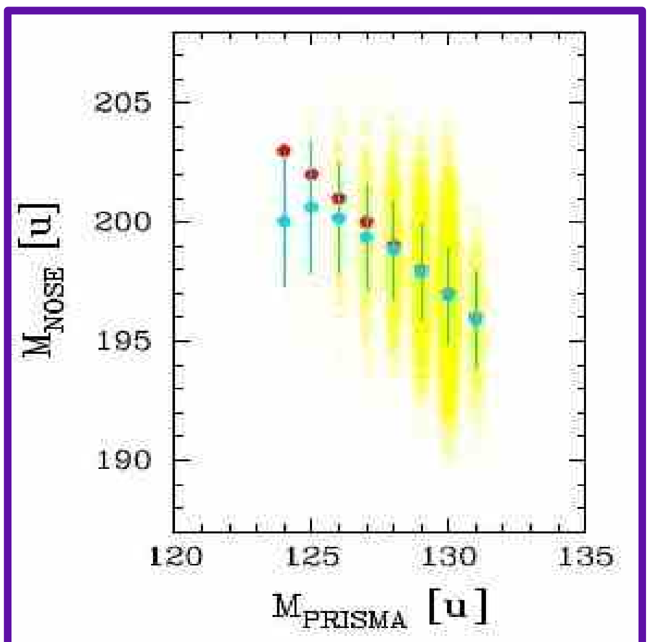

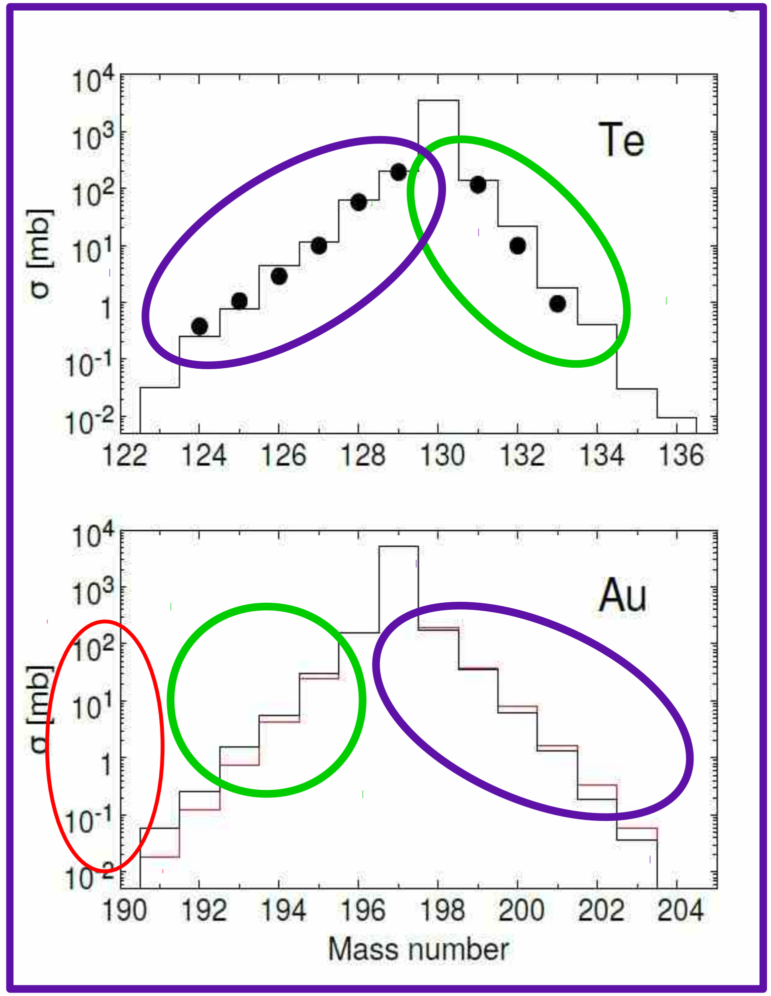

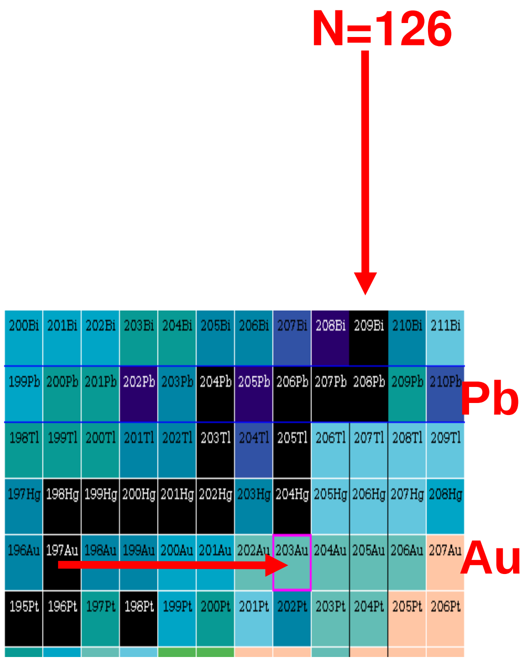

Multinucleon transfer reactions are a suitable tool for the production of heavy neutron-rich nuclei

Te isotopes with “more” neutrons than in ^{130}Te

Au isotopes with “more” neutrons than in ^{197}Au

$^{94}Rb+^{208}Pb$: MNT with neutron-rich beam

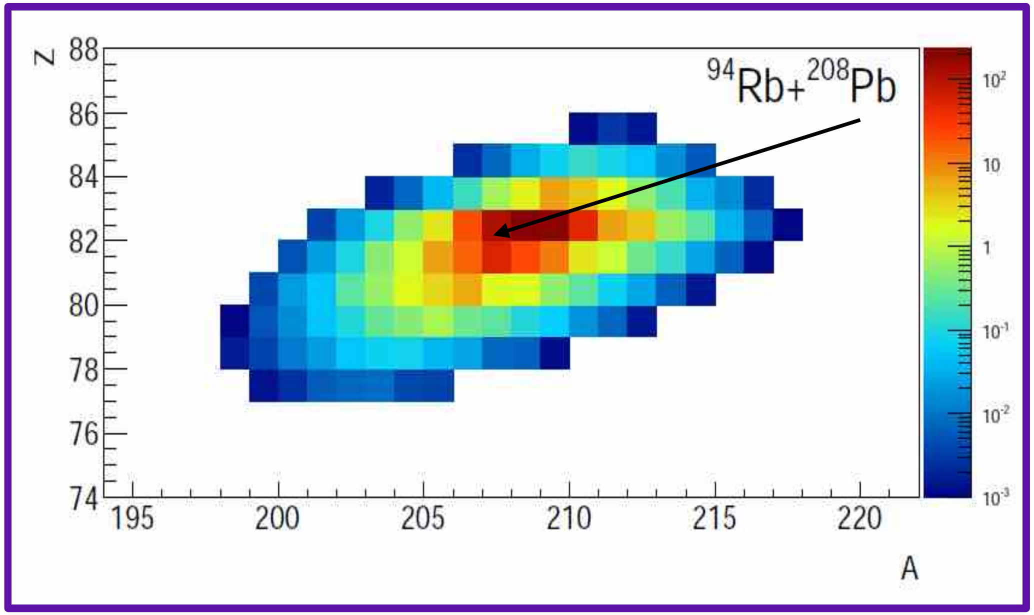

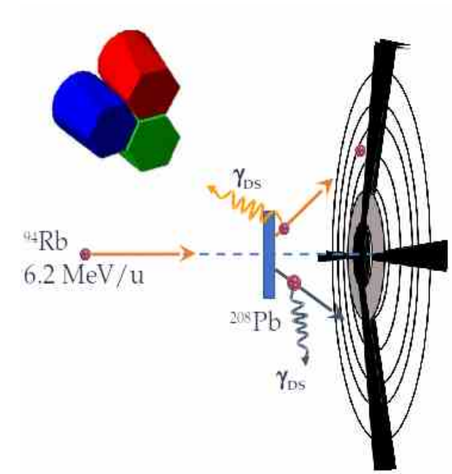

ISOLDE – CERN: MINIBALL + CD particle detector → fragment-gamma(-gamma) coincidencies

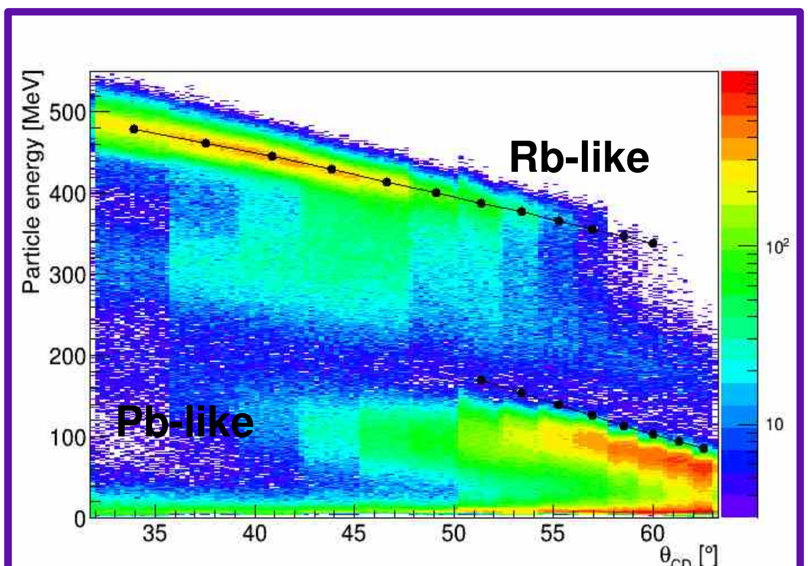

P. Čolović et al. PRC 102 (2020) 054609
Population of lead isotopes in binary reactions using a 94Rb radioactive beam

ISOLDE EXP IS572, spokespersons:
J.J. Valiente Dobon and S. Szilner

$^{94}Rb+^{208}Pb$: MNT with neutron-rich beam

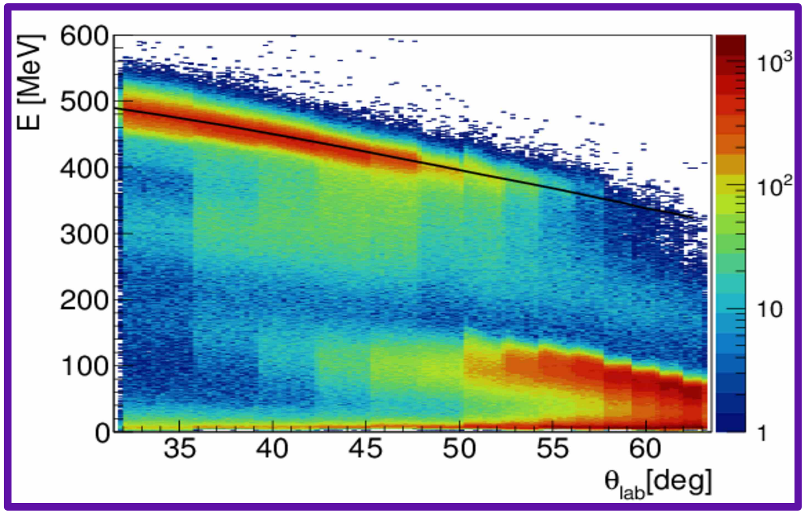

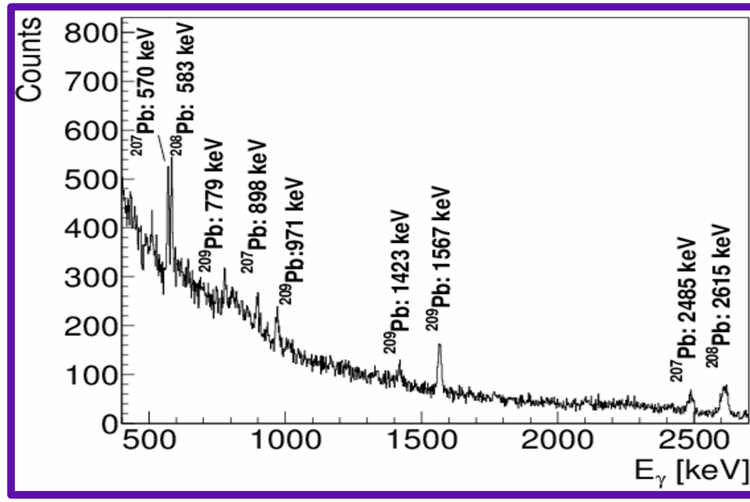

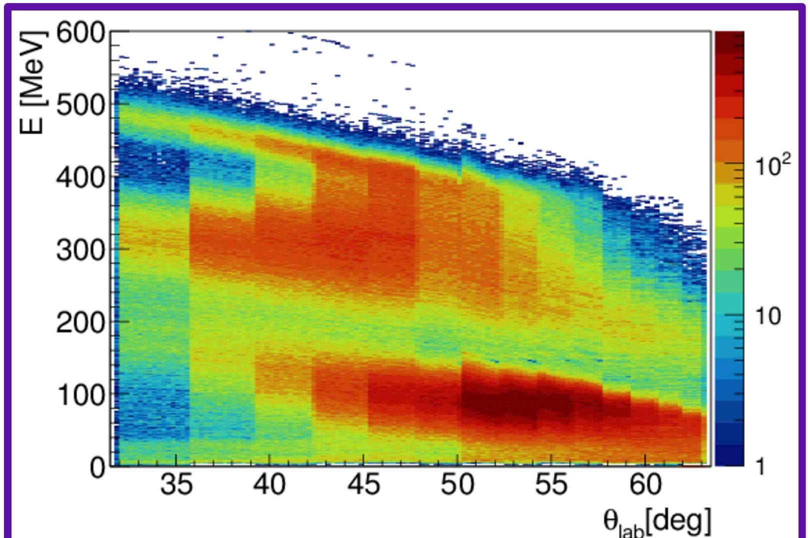

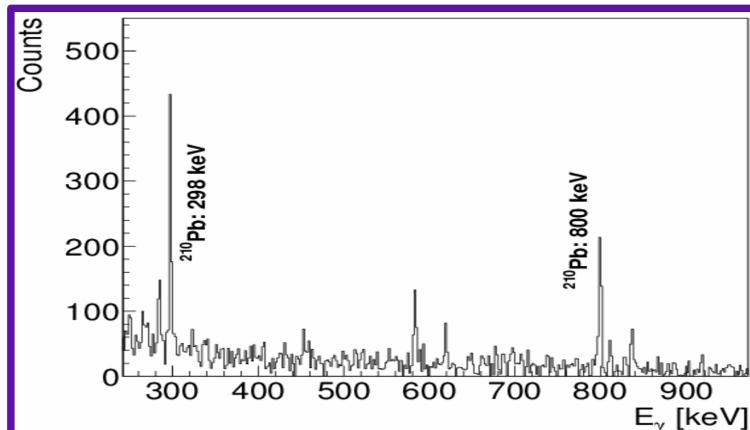

Matrix of total kinetic energy vs angle → fragments (top) and fragments-gamma coincidencies (bottom)

Prompt, up to 200 ns (top), and delayed, up to 2μs (bottom) γ -ray spectra taken in coincidence with the Rb-like detected in CD detector

$^{94}Rb+^{208}Pb$: MNT with neutron-rich beam

^{208}Pb

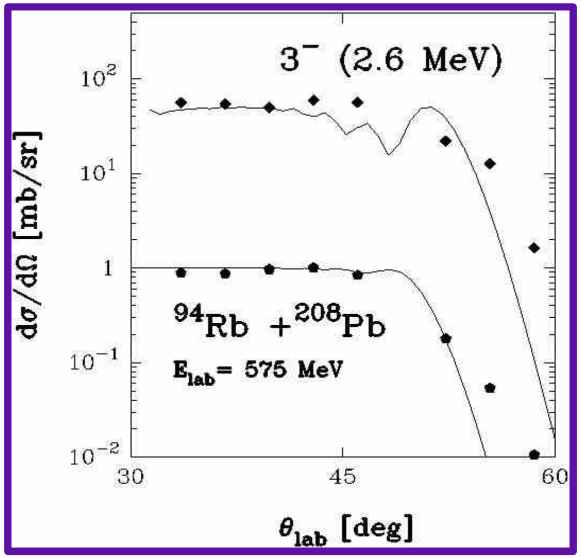

Differential cross sections for the inelastic scattering of the 3^- state in ^{208}Pb. Data have been normalized at forward angles to the DWBA calculation.
Experimental quasi-elastic cross sections and theoretical elastic scattering, divided by Rutherford cross section.

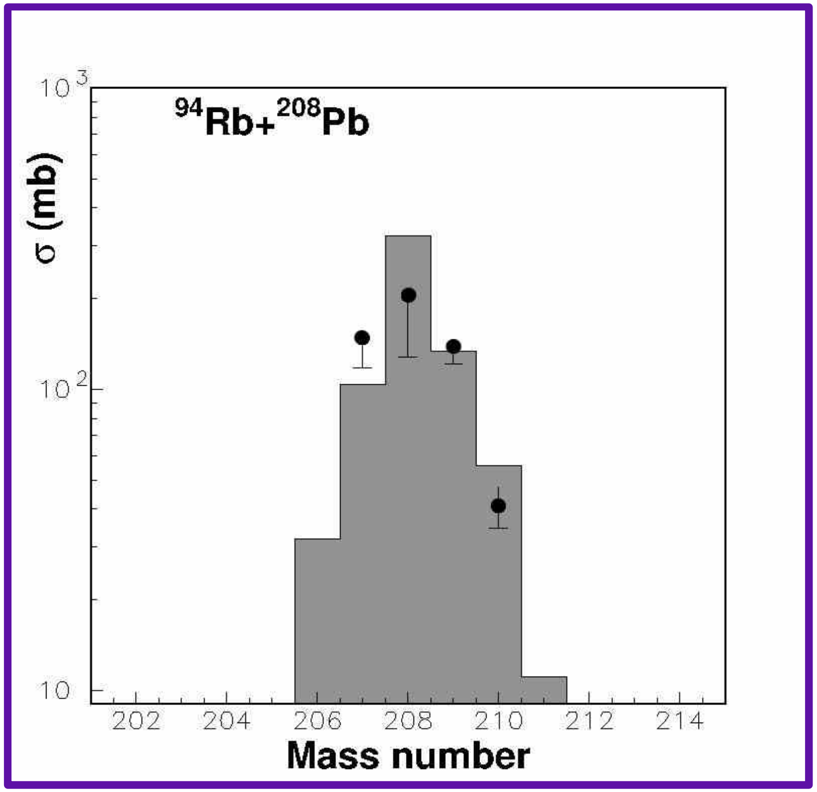

Total cross sections of Pb isotopes compared with the GRAZING calculations. The measured cross sections are indicated as lower limits, while those which include the estimated values for the ground states are indicated with full points.

P. Čolović et al. PRC 102 (2020) 054609

$^{94}Rb+^{208}Pb$: MNT with neutron-rich beam

GRAZING calculated total cross sections for Pb isotopes in $^{94}Rb+^{208}Pb$ and $^{87}Rb+^{208}Pb$ reactions

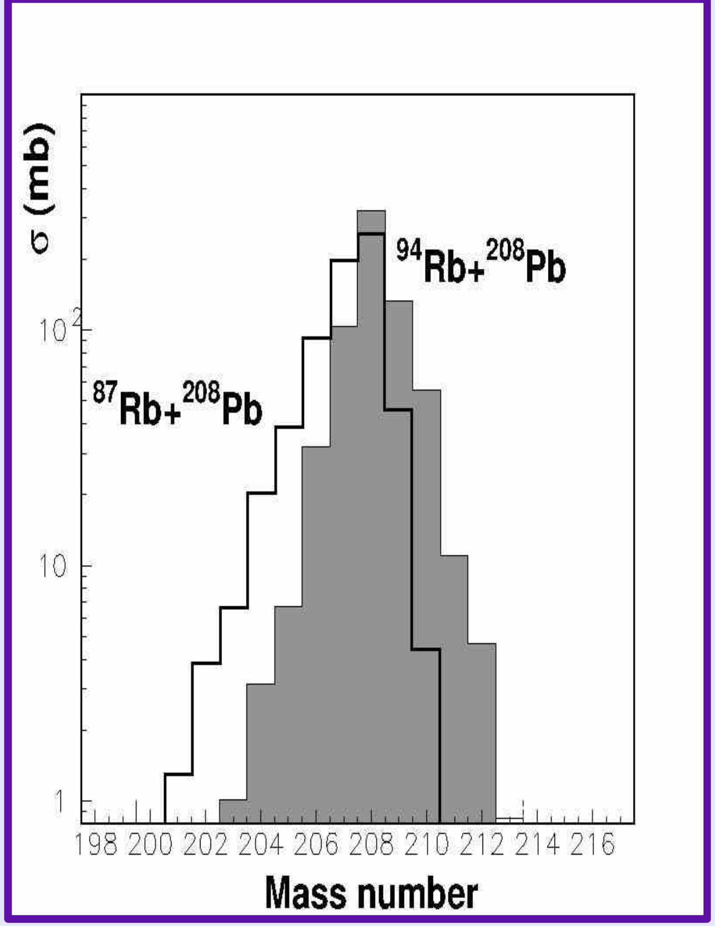

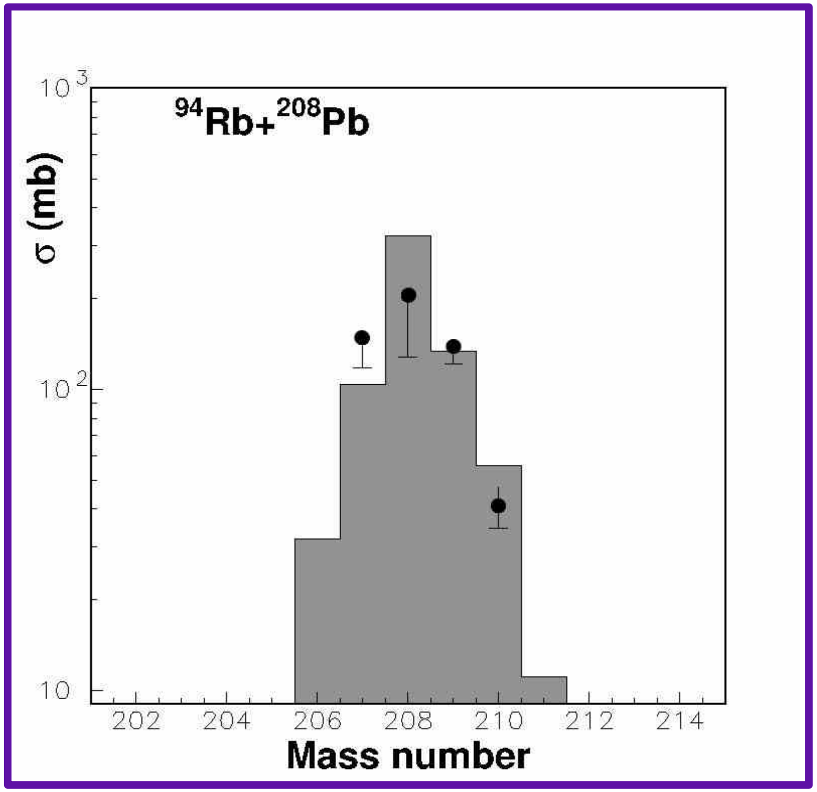

Total cross sections of Pb isotopes compared with the GRAZING calculations. The measured cross sections are indicated as lower limits, while those which include the estimated values for the ground states are indicated with full points.

P. Čolović et al. PRC 102 (2020) 054609

What new directions could stable ion beams and novel instrumentation bring to further our understanding of dynamics through gamma-ray spectroscopy?

$$N_{\text{detected}} = j_{\text{beam}} \cdot N_{\text{target}} \cdot \frac{d\sigma}{d\Omega} \cdot \Delta\Omega \cdot \epsilon_{\text{eff}}$$

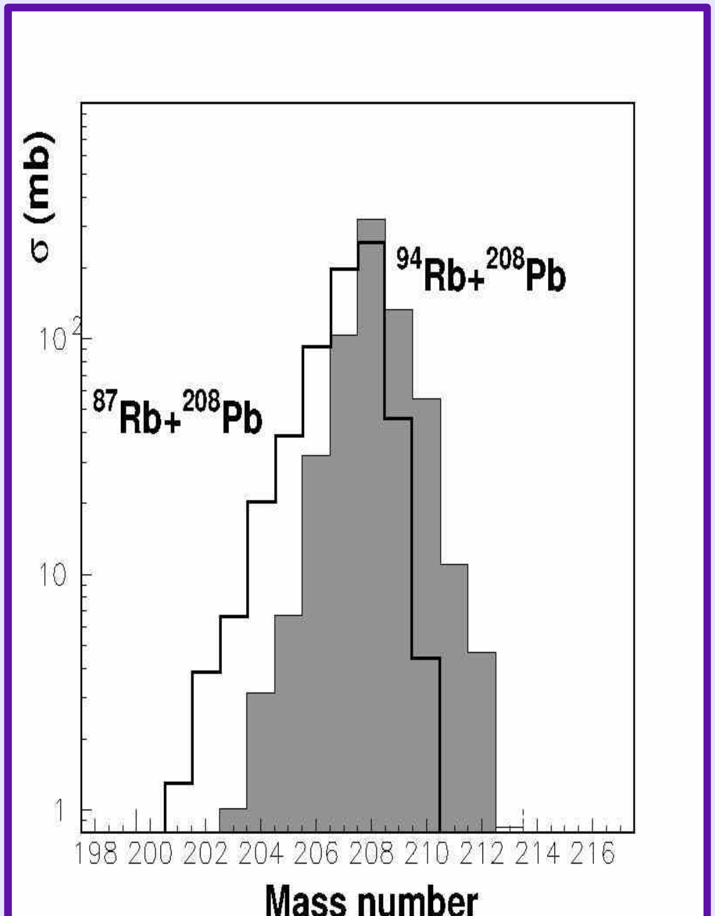

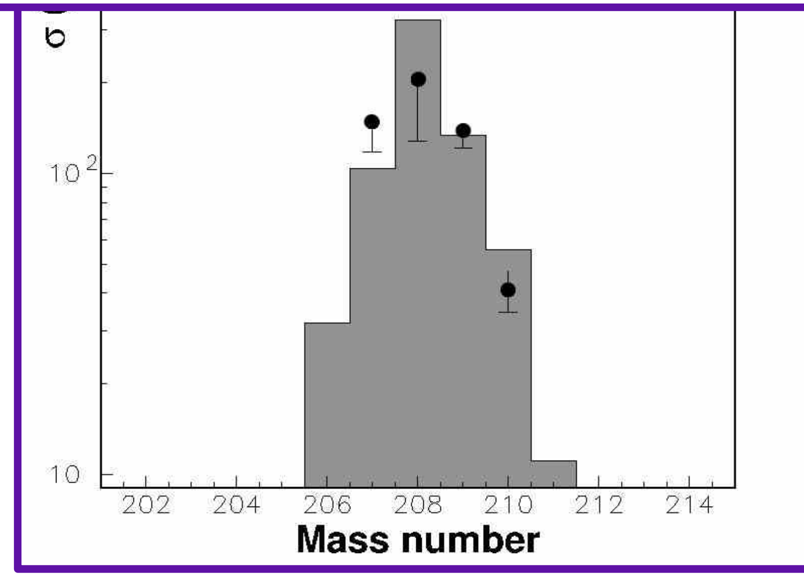

Total cross sections of Pb isotopes compared with the GRAZING calculations. The measured cross sections are indicated as lower limits, while those which include the estimated values for the ground states are indicated with full points.

P. Čolović et al. PRC 102 (2020) 054609

What new directions could stable ion beams and novel instrumentation bring to further our understanding of dynamics through gamma-ray spectroscopy?
Excited states in yttrium isotopes

transfer reactions: $^{90}Zr+^{208}Pb$, fragment – gamma coincidences (PRISMA + CLARA)

→ fragment – gamma coincidences: new gammas uniquely attributed to the specific isotope, the isotopic chain populated in the same reaction, relatively high spin states

M. Varga Pajtler et al, Phys. Scr. 96 (2021) 035305 and Ph.D. Thesis University of Zagreb (2014)

fission of ^{238}U accelerated in inverse kinematic on ^{9}Be, fragment – gamma coincidences (VAMOS + AGATA + EXOGAM)

→ fragment - gamma - gamma coincidences: the larger efficiency of arrays for mutual gamma coincidences

J.H. Kim et al, Eur. Phys. J. A 53 (2017) 162

fission of ^{235}U induced by cold neutrons, gamma coincidences (EXILL gamma spectrometer)

→ prompt and delayed gammas, spins suggested by the gamma angular correlation analysis

W. Iskra et al, Phys. Scr. 92 (2017) 104001

Excited states in yttrium isotopes

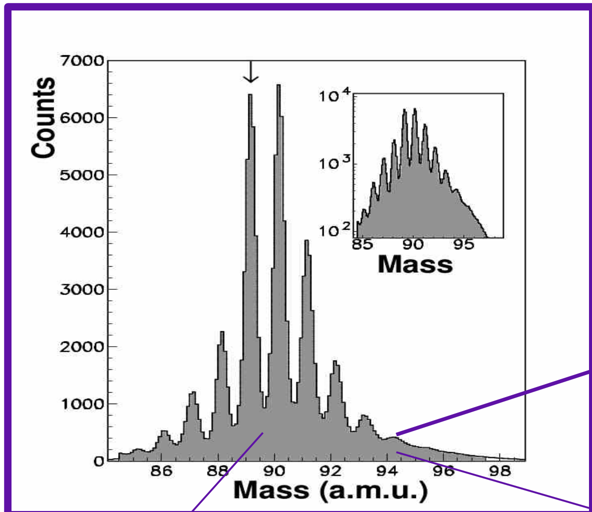

94Y

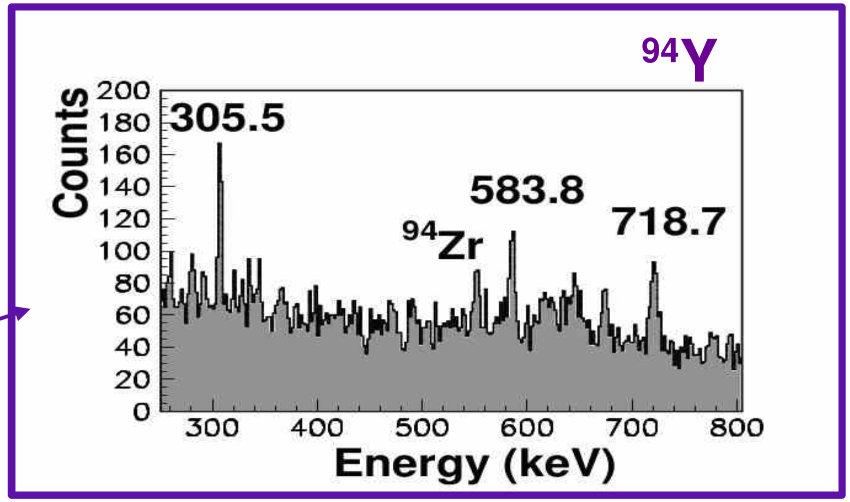

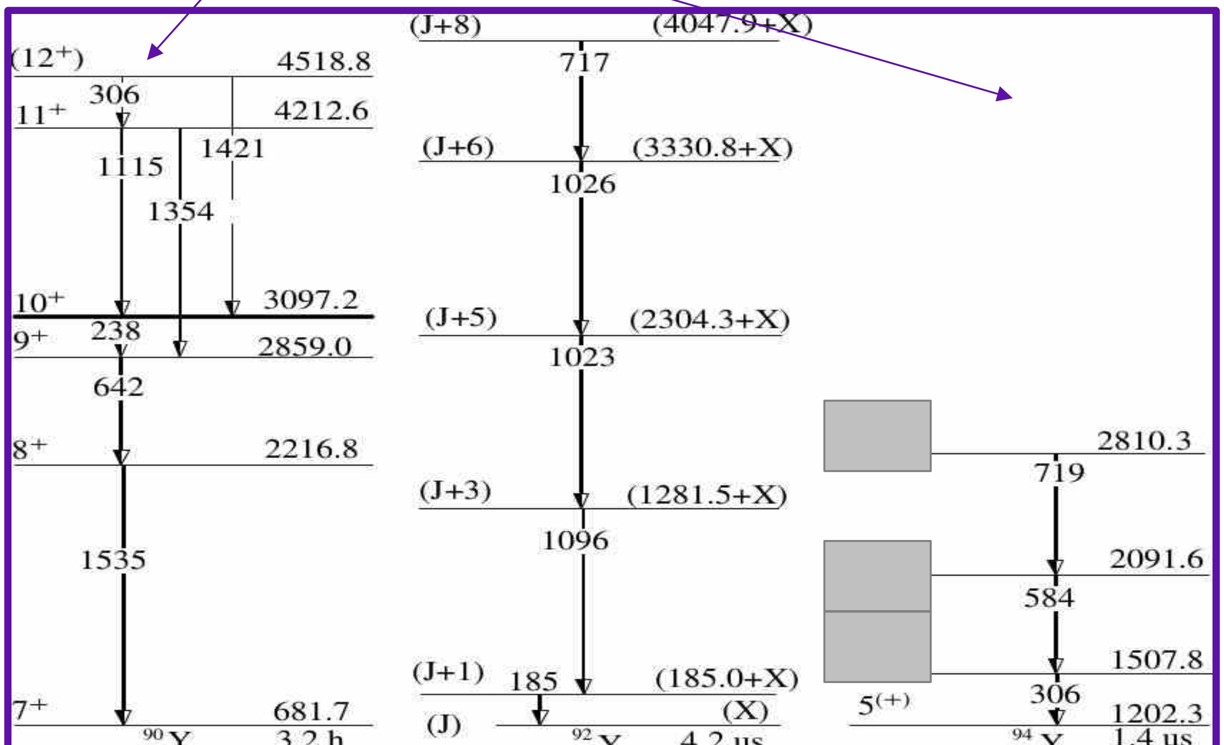

90Y 92Y 94Y

transfer reactions: $^{90}Zr+^{208}Pb$, fragment – gamma coincidences (PRISMA + CLARA)

fission of ^{238}U accelerated on ^{9}Be, fragment – gamma - gamma coincidences (VAMOS + AGATA + EXOGAM)

Excited states in yttrium isotopes

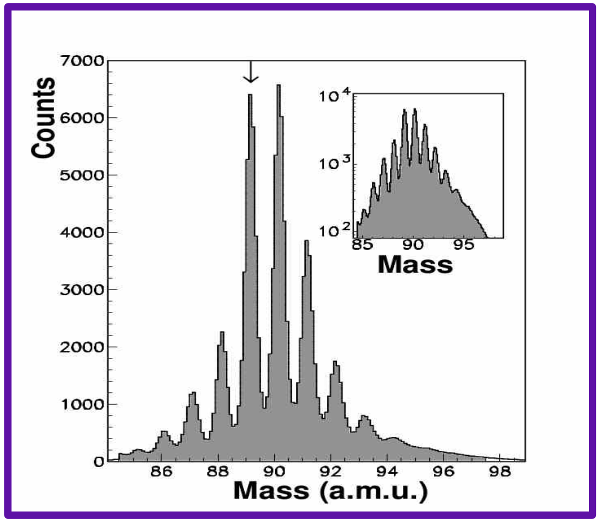

transfer reactions: $^{90}Zr + ^{208}Pb$, fragment – gamma coincidences (PRISMA + CLARA)

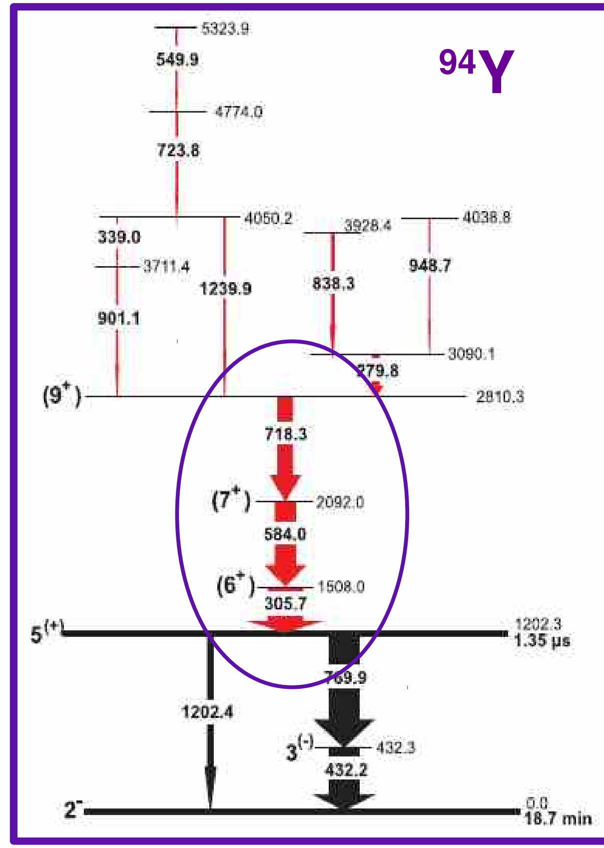

fission of ^{235}U: mutual coincidences, prompt and delayed gammas, spins suggested by the gamma angular correlation analysis (EXILL gamma spectrometer)

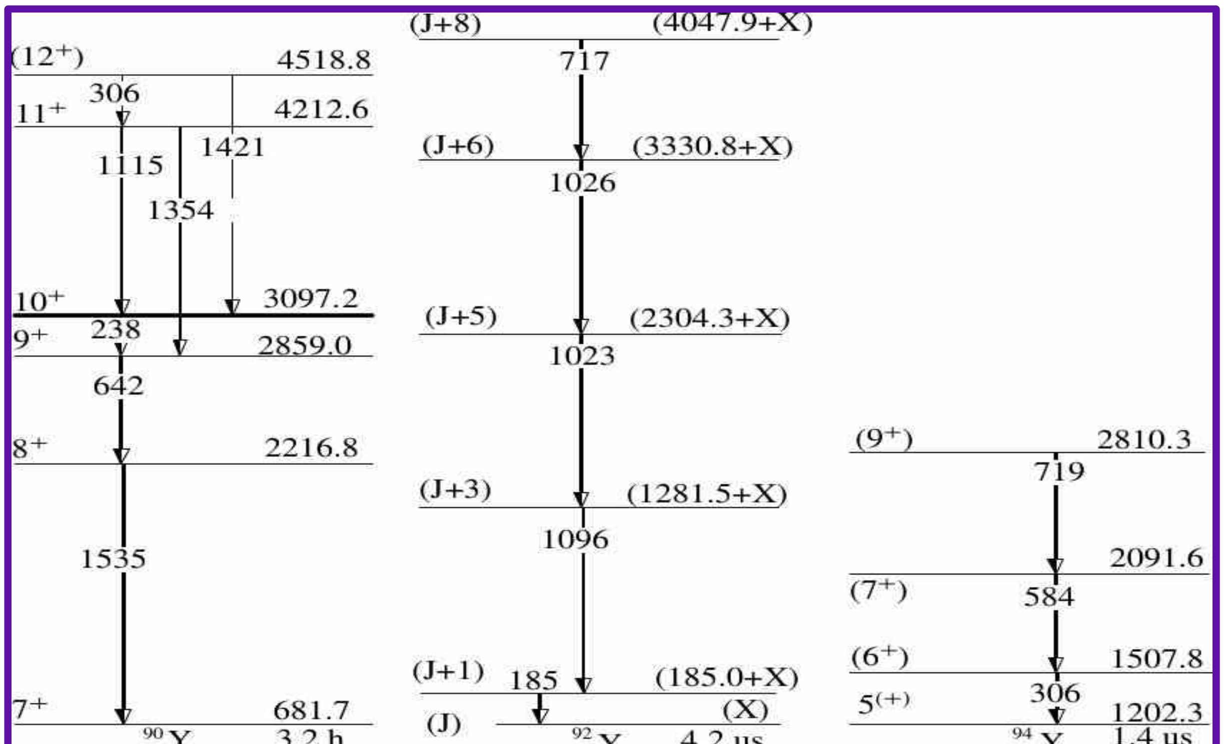

90Y 92Y 94Y

L. Corradi, G. Pollarolo, J. Diklić, T. Mijatović, F. Galtarossa, P. Čolović, A. Goasduff, D. Montanari, E. Fioretto, A.M. Stefanini, G. Montagnoli, G. Coucci, F. Scarlassara, J.J. Valiente-Dobon, D. Mengoni, D. Jelavić Malenica, N. Soić, N. Vukman, M. Milin, D. Nurkić and CLARA-AGATA collaboration

Ruđer Bošković Institute, Zagreb, Croatia
INFN - Laboratori Nazionali di Legnaro, Legnaro, Italy
INFN and Universita di Torino, Italy
INFN and Universita di Padova, Padova, Italy
University of Zagreb, Croatia
ISOLDE, CERN

This work was partly supported by the Croatian Science Foundation under the project IP-2018-01-1257.

Kokopelli: links distant and diverse communities together.